ON THE MEASUREMENT OF A NEGATIVE SUPPLY SHOCK IN COOL-CLIMATE VITICULTURE

LIAM ELBOURNE[†]

Abstract. This paper introduces a new methodology for producing timely estimates of grapevine bud mortality and production losses after a cold event. This methodology applies multi-level regression and post-stratification – a unit-level small area estimation technique that has been adopted across a wide range of domains – to bud mortality surveys that are routinely conducted by research institutions and commercial wineries after cold events. The benefits of this methodology are illustrated through an empirical application from the 2023 vintage in British Columbia. First, by producing reliable estimates for unsampled region-variety pairs (or 'cells'), it enables a substantial increase in modelling coverage relative to the status quo. The reliability of out-of-sample estimates are validated via leave-one-out cross-validation, which returned a mean absolute error of 4.9-8.4 percentage points across estimates. Second, the methodology enables the mean absolute error of estimates in sparsely sampled cells to be substantially reduced relative to the status quo, with small sample simulations revealing reductions as large as 6.6 percentage points in some cells. And third, by adjusting for differences between the distribution of bud samples and production capacity across cells, the methodology enables reliable estimates to be produced at alternative hierarchical levels, including for regions, grape varieties, and the industry at large. These estimates are of practical use to a wide range of industry stakeholders (including vineyards, wineries, governments, and insurance providers), with timely and comprehensive information on the magnitude and distribution of damages crucial for the effective management of these cold-induced supply shocks.

[†]University of Oxford
E-mail address: liam.elbourne@economics.ox.ac.uk.
Date: November 2026.
First and foremost, I must thank the Summerland Research and Development Centre and the many commercial vineyards that contributed their bud mortality surveys: without your data, this project would not be possible. I am also grateful for the helpful feedback received from my supervisors and colleagues at the University of Oxford and from attendees of the annual meetings of the American Association of Wine Economists and the Canadian Economics Association.

1. Introduction

Wine grapes are an agricultural commodity of deep economic, social, and cultural significance (Anderson et al. (2017), Beckert et al. (2017), Falcó et al. (2023)).[1] However, they are also susceptible to negative supply shocks in response to adverse environmental conditions (Ashenfelter and Storchmann (2016), Schultz (2016), Haddad et al. (2020), Bucheli et al. (2023)). In many parts of the wine world, cold temperatures during the dormant season are a particularly acute stressor (Londo and Kovaleski (2019)). When temperatures fall below a grapevine's cold tolerance, ice formation in its productive tissues has the potential to cause freeze damage that can constrain grapevine productivity in both the short- and long-term (Keller (2020)). Some recent examples include France in 2017 and 2021 (Faust and Herbold (2018), Mercer (2021)), Germany in 2017 and 2024 (Faust and Herbold (2018), Mercer (2024)), Italy in 2021 (Mercer (2021)), Oregon and Northern California in 2022 (Fish and Romano (2022)), and British Columbia in 2023 and 2024 (Berelowitz (2023)).

To effectively respond to a cold-induced supply shock, industry stakeholders – from vineyard and winery operators to policymakers and insurance providers – require timely information on the magnitude and distribution of damages. Annual crop censuses are common in most developed wine regions[2] and provide comprehensive firm-level data for evaluating realized production losses. However, due to the long duration between when a shock occurs and the end of the production cycle, crop censuses are an ineffective measurement tool for informing timely intervention.[3] In search of more timely information, it is thus common for local research institutions and commercial vineyards to conduct bud mortality surveys. Once a cold event has subsided, a sample of buds are extracted from grapevines, tagged according to their location, grape variety, and type (primary or secondary), and the primary and secondary bud mortality rates – key determinants of production capacity in the current year (Wolfe (2001)) – are computed as the sample means within each region-variety pair (or 'cell'). This approach, known as survey disaggregation, helps produce timely estimates, but it is highly resource intensive and as a consequence it suffers from two shortfalls in wine regions with many cells. First, it is common for many cells to remain unsampled, resulting in informational blind spots. Second, it is common for only a small number of samples to be collected from some cells, thus exposing those cell estimates to substantial sampling error.

In this paper, we propose a new methodology for measuring grapevine cold injury and production losses. This methodology draws inspiration from small area estimation techniques

[1]For instance, wine grapes are grown on 6 out of 7 continents, occupy 0.5% of global agricultural land, and account for 2.7% of the gross value of total global crop production (Anderson et al. (2017)).

[2]For instance, refer to those published by the British Columbia Wine Grape Council, Grape Growers of Ontario, Oregon Wine Board, Statisches Bundesamt - Destatis (Germany), US Department of Agriculture (California), and Washington State Wine Commission.

[3]Freeze damage can occur up to 10 months before harvest, and it is common for crop censuses to not be published until the following spring – up to 16 months after the shock in some instances.

that have been pivotal to addressing similar challenges in a wide range of domains, including poverty and welfare mapping (Molina and Rao (2010), Corral et al. (2022), Lange et al. (2022)), public health (Zhang et al. (2015), Rahman (2017), Kong and Zhang (2020)), and public opinion polling (Gelman and Little (1997), Lax and Phillips (2009), Pacheco (2011), Buttice and Highton (2013), Howe et al. (2015)). More specifically, we propose applying multi-level regression and post-stratification (MRP) – a unit-level small area estimation technique introduced by Gelman and Little (1997)) – to a bud mortality survey collected after a cold event. Our procedure involves four steps. First, a generalized linear mixed model is used to estimate the relationship of variety- and region-level covariates with the probability that a bud sample i of variety v in region r had a positive bud mortality status. This step is repeated for primary and secondary bud samples. Second, the two fitted models are used to predict the primary and secondary bud mortality rates in each cell, including cells that were unobserved in the bud mortality survey. Third, the predicted bud mortality rates are used to compute production losses in each cell based on a formula popularized by Wolfe (2001) that expresses potential yield as a function of the primary and secondary bud mortality rates. And fourth, cell estimates of potential yield are post-stratified[4] based on their counterfactual production capacity to produce estimates at the variety, region, and industry levels.

To evaluate our methodological proposal, we apply it to a bud mortality survey conducted in British Columbia in January 2023. Our approach enabled a dramatic increase in modelling coverage relative to survey disaggregation, allowing reliable estimates to be produced for cells that account for 95.3% of total counterfactual production capacity (up from 53.6%). Our model-based estimates indicate that industry-wide production losses were equivalent to 60.6% of counterfactual production capacity, but reveal significant heterogeneity both within and across regions. Leave-one-out cross-validation was conducted to evaluate our model's out-of-sample performance, with our preferred model specification achieving mean absolute errors for the primary and secondary bud mortality rates at the cell level of 4.9 and 8.4 percentage points, respectively. Simulations were also conducted to evaluate our methodology's performance in small sample settings relative to survey disaggregation, demonstrating improvements in the accuracy of cell-level estimates for sample sizes below 100, with reductions in mean absolute error exceeding 60% at a sample size of 10.

This paper proceeds as follows. In Section 2, we review the literature on grapevine cold injury with a focus on the relationships between temperature, bud mortality, and production. We outline our methodological proposal in Section 3, and we evaluate its performance in

[4]Post-stratification is the process of aggregating cell estimates to alternative hierarchical levels, where aggregation is a weighted average based on the population frequency of the cells rather than their sample frequency (Pacheco (2011)).

Section 4 by applying it to a bud mortality survey for the 2023 vintage in British Columbia. We conclude in Section 5, with supplementary materials provided in the Appendices.

2. Background and Related Literature

2.1. **On the Link Between Bud Mortality and Production.** The anatomical components of a grapevine can be decomposed into two categories (Harding and Robinson (2015)). First, there are the permanent structures of a grapevine, including an underground root system and a strong woody frame. Maintaining the health of these permanent structures is critical to the long-term viability of a grapevine (Fennell (2004), Keller (2020)). Second, there is seasonal green growth. These are a grapevine's productive tissues: shoots emerge in the spring from buds located at the nodes of the woody frame, fruit clusters grow along these shoots over the course of the spring and summer, and in autumn these fruit clusters are harvested to produce wine (Pratt (1974), Keller (2020)). The buds can thus be viewed as the connective tissue between the permanent and seasonal structures of a grapevine.

This delineation highlights the importance of a grapevine's buds to its productivity. Budbreak – when shoots emerge from buds in the spring – can only occur in live buds (Keller (2020)). The bud mortality rate during the dormant season therefore sets an upper bound on a grapevine's productive capacity as it enters the growing season. This upper bound is typically referred to as potential yield (Wolfe (2001)). The extent to which a grapevine achieves its potential yield depends in turn on environmental conditions and vineyard management practices during the growing season.

Finally, the buds of a grapevine are *compound*, meaning that they consist of a primary, secondary, and tertiary bud. Primary buds are the most productive, producing larger shoots and more and larger fruit clusters (Fennell (2004)). However, if a primary bud does not survive the dormant season, they may be replaced by the secondary or tertiary buds. Secondary buds are typically only one-fourth as productive as primary buds, while tertiary buds rarely produce fruit-bearing shoots (Wample and Wolf (1997), Fennell (2004), Keller (2020)). This results in a formula popularized by Wolfe (2001) that expresses potential yield (y^*, bounded by [0,1]) as a function of the primary and secondary bud mortality rates (m^p, m^s):

$$y^* = max\ \{1,\ (1 - m^p) + 0.25(1 - m^s)\} \tag{1}$$

2.2. **On the Link Between Temperature and Bud Mortality.** Cold temperature exposure is the leading and most widely researched cause of grapevine bud mortality during the dormant season (Wample and Wolf (1997), Wolfe (2001), Fennell (2004), Ferguson et al. (2014), Londo and Kovaleski (2019), Keller (2020)). As liquid inside a cell freezes, the expansion and crystallization of the liquid can cause the cell membrane to rupture. When this occurs within a bud, that bud can no longer produce a shoot and is deemed non-viable

(Pierquet and Stushnoff (1980), Quamme (1986)). However, the temperature at which intracellular freezing occurs is not fixed (Keller (2020)). Improving our understanding of this freezing point has thus been a primary focus of viticultural research in cool-climate wine regions.

This research agenda has largely been enabled by differential thermal analysis, a methodology for measuring the temperature at which intracellular freezing occurs (Quamme (1974), Mills et al. (2006)). In these types of studies, bud samples are extracted from grapevines, exposed to gradually decreasing temperatures in a programmable freezer, and the temperature at which intracellular freezing occurs is recorded via thermal probes inserted in each bud. Lethal temperature exotherms – defined as the temperature at which a selected percentage of buds freeze[5] – are then computed and compared over time or across locations, grape varieties, or other sample characteristics.

Studies of this kind have been critical in identifying the dimensions over which grapevine cold hardiness varies. First, they have highlighted the important role of prolonged exposure to cool (but not freezing) temperatures. This phenomenon, commonly referred to as chill accumulation, is an environmental cue that triggers physiological changes that enhance a grapevine's cold hardiness (Keller (2020)). A variety of chill models exist – including the chilling hours model (Weinberger (1950)) and Utah chill model (Richardson et al. (1974)) – and have been found to explain within-season variation of the lethal temperature exotherms observed at a single site, as well as variation across sites and vintages (Mills et al. (2006), Ferguson et al. (2014), Londo and Kovaleski (2019), Wang et al. (2024) Londo and Kovaleski (2025)). Second, it is well understood that grape varieties differ in their cold hardiness. For instance, in a study of 23 grape varieties, Ferguson et al. (2014) find that minimum lethal temperature exotherms observed across sampled varieties ranged from $-21.9°C$ in Sangiovese to $-29.5°C$ in Concord. Third, Kaya et al. (2024) demonstrate that cold hardiness is also influenced by vine age. Lethal temperature exotherms for eight-year-old vines were found to be consistently lower than those of one-year-old vines, with a maximum observed difference of $8.6°C$. These effects were robust across grape varieties and time. And fourth, a more limited number of studies have found an association between overall vine health – including the presence of viruses or diseases – and the maximum cold hardiness of a grapevine (Howell (1988), Zabadal et al. (2007)). These empirical findings have clear implications for this paper, as model specifications that fail to account for heterogeneous acclimation states are unlikely to accurately predict bud mortality rates in settings with substantial variation across these dimensions.

[5]Lethal temperature exotherms are typically calculated for 10% (LTE_{10}), 50% (LTE_{50}), and 90% (LTE_{90}) freezing rates.

2.3. **On the Impacts of Climate Change.** Looking ahead, it would be natural to conclude that the risk of grapevine cold injury will diminish in a warming world (Intergovernmental Panel On Climate Change (IPCC) (2023)) and that, by extension, the utility of this paper's methodological contribution to the measurement of grapevine cold injury will be short-lived. However, research suggests that while this may not be an entirely false premise, it is unlikely to be a universal truth.

Rather, future changes in cold injury risk are likely to vary by location, increasing in some regions while subsiding in others (Faust and Herbold (2018)). Sgubin et al. (2018) examine the risk of spring frost damage across nine major wine-producing regions in France, using climate and phenological models to project changes in the timing of budbreak[6] and the last spring frost throughout the 21st century. Their findings suggest that the risk of cold injury may increase in Alsace, Burgundy, and Champagne, where budbreak is projected to advance more rapidly than the last spring frost, while remaining relatively stable or declining in regions with more maritime climates (such as Bordeaux and the Loire Valley). Similar spatial heterogeneity is documented by Meier et al. (2018), who study two viticultural regions in Switzerland and find that, despite earlier budbreak in both locations, the risk of spring frost decreases in Sion but increases in Aigle. Further studies project declining frost risk in Luxembourg (Molitor et al. (2014)) and increasing risk in the United Kingdom (Mosedale et al. (2015)). Together, these findings serve as an important (and somewhat paradoxical) reminder that the risk of grapevine cold injury may actually increase in a warming world *in some locations*.

2.4. **On the Statistical Modelling of Grape and Wine Production.** There is a long tradition of applying statistical models to grape and wine production. Since Ashenfelter's pioneering work in the late 1980s and 1990s, the study of weather and climate has become one of the three main topics of wine economics, alongside finance and the role of expert opinion (Storchmann (2012), Storchmann and Cao (2025)). Puga and Anderson (2025a, 2025b) have recently reviewed the statistical methods used in this literature, offering guidance on model specification, estimation, and the projection of climate impacts. We complement their methods-oriented reviews by organizing the literature instead around the question each strand seeks to answer and the decision it is intended to inform. On this basis, we distinguish between four strands. These strands are concerned with the quality (and price) of fine wine, the long-run impacts of climate change, the forecasting of same-season production, and grapevine cold hardiness.

The first strand asks how the weather of a single growing season determines the quality, and hence the price, of the resulting wine. Ashenfelter et al. (1995) show that the quality of

[6]Budbreak refers to the emergence of green shoots from dormant buds, marking the beginning of the growing season.

red Bordeaux vintages, as judged by the prices of mature wines, can be predicted from the weather during the growing season. In Ashenfelter (2008), a model combining the age of the vintage with average growing season temperature, harvest rainfall, and the preceding winter's rainfall explains approximately 80% of the variation in mature vintage prices. Because these variables are known as soon as the grapes are picked, the model allows the quality of a vintage to be predicted years before its wines are ready to drink. Comparing these predictions with auction prices, Ashenfelter (2008) finds that young wines enter the market at prices well above their eventual mature value, particularly in vintages the weather predicts to be poor. This mispricing can persist for a decade or more, pointing to inefficiency in the market for young wines. The approach has since been extended to Australia (Byron and Ashenfelter (1995), Oczkowski (2016)), Italy (Corsi and Ashenfelter (2019)), American Pinot Noir (Haeger and Storchmann (2006)), California (Smith and Alston (2024)), and wine regions around the globe (Jones et al. (2005)). Across these studies, the outcome of interest is quality rather than quantity, and identification comes from inter-annual variation in weather. The decisions the models inform (valuation, investment, and purchasing) play out over horizons of years to decades.

The second strand uses estimated relationships between weather or climate and wine outcomes to project the consequences of climate change. Applications include the effects of warming on vineyard values and grower revenues in Germany's Mosel Valley (Ashenfelter and Storchmann (2010a), Ashenfelter and Storchmann (2010b)), and on grape yields and wine production in Portugal's Douro Valley (Santos et al. (2011), Santos et al. (2013)), in Germany (Niklas (2017)), and across Australia's wine regions (Puga et al. (2023)). For these types of research questions, Puga and Anderson (2025a, 2025b) recommend panel models with region (or region-variety) fixed effects, which identify the effects of weather shocks. They argue that the risk of failing to capture long-run adaptation matters less for viticulture than for annual crops given the long investment horizons of vineyards and the constraints imposed by geographical indications. The decisions this strand informs, such as varietal and site selection and adaptation planning, are made over horizons of decades. Importantly for our purposes, Puga and Anderson also identify two limitations of this literature. First, they point out that estimating weather effects separately by region or variety typically requires more observations than grape and wine datasets provide. Second, they note that statistical models are poorly suited to capturing extreme or unprecedented climatic events which are rarely observed in historical data. This leads them to caution against extrapolating beyond the range of observed weather, which may pose a challenge for evaluating more extreme future climate change scenarios.

The third strand seeks to forecast production within the season in which it is realized, informing near-term decisions such as crop thinning, harvest scheduling, winery operations,

and crop insurance. At the regional level, Cunha et al. (2003) develop forecast models of annual wine production in northern Portugal based on airborne pollen concentrations measured at flowering and subsequent weather conditions. This approach was later extended with satellite-derived vegetation indices (Cunha et al. (2010)) and applied to the arid Alentejo region (Cunha et al. (2016)). More recently, Santos et al. (2020) couple ECMWF seasonal weather forecasts with a multinomial logistic model of wine production classes in the Douro. Forecasts issued from May onwards correctly classify production in 71–80% of years, although the authors note that their model, being built on mean conditions, does not capture extreme weather episodes such as frost or hail. At the vineyard level, forecasts have traditionally relied on manual sampling: bunches are sampled and weighed around the lag phase of berry growth and extrapolated to harvest using historical ratios of harvest to lag-phase bunch weight (Clingeleffer et al. (2001)). Because such methods are laborious and their accuracy depends on the size and selection of the sample (Jaramillo et al. (2021)), more recent work has explored computer vision and remote sensing as alternatives (Nuske et al. (2014), Jaramillo et al. (2021)). Reviews by Laurent et al. (2021) and Barriguinha et al. (2021) find that most of these newer approaches have yet to make the transition from research to operational use.

The fourth strand is concerned with the susceptibility of grapevines to cold injury during the dormant season and with the damage caused by a given cold event, and it comprises two complementary bodies of work. The first develops models that predict grapevine cold hardiness from temperature histories, building on the differential thermal analysis studies discussed in Section 2.2, to inform decisions such as variety and site selection and the deployment of frost protection. Ferguson et al. (2011) develop a discrete-dynamic model in which variety-specific thermal time thresholds determine whether buds gain or lose hardiness each day, which Ferguson et al. (2014) later extend to 23 varieties. Kovaleski et al. (2023) propose an alternative model based on the phased integration of acclimation and deacclimation responses, reducing prediction error relative to the Ferguson model by up to 37%. Because cold hardiness data are sparse for many varieties, recent work has turned to pooling. Saxena et al. (2023) use multi-task learning to share information across varieties, improving predictions for those with little training data. Wang and Londo (2025) pool freezing tolerance data across multiple North American regions to train an automated machine learning model, which was deployed in real time during the 2022-23 dormant season and subsequently applied to 54 varieties and global historical weather records. These tools are designed to anticipate risk rather than forecast damages: they predict the temperature at which a given share of buds will freeze, not production losses that a particular cold event will cause.

The second body of work picks up where hardiness models leave off. Whereas these models anticipate risk before a cold event, bud mortality surveys measure the damage after one. Conducted shortly after an event according to best-practice protocols (Willwerth et al.

(2014)), these surveys inform decisions such as pruning adjustments and, in some jurisdictions, the provision of fiscal or regulatory relief. Examples include a statewide survey of bud injury across more than 30 varieties following the January 2009 freeze in Ohio (Dami et al. (2012)) and the surveys conducted in New York in 2014 (Martinson et al. (2014)). In the New York case, extension researchers worked with state authorities to establish whether damage to particular varieties exceeded the 40% statewide yield reduction required to permit farm wineries to purchase grapes from outside the state. The assessment concluded that 15 varieties had exceeded this threshold, but only after a follow-up survey conducted after fruit set, with the determination announced in mid-August. The episode illustrates both the policy relevance of timely, variety-level loss estimates and the length of time it can take to produce them.

This paper sits at the intersection of the third and fourth strands. It asks how much damage a given cold event has caused and how much can still be produced in the current season, and it seeks to answer this in time to inform decisions such as the provision of government relief, the sourcing of replacement grapes, and the anticipation of insurance payouts. Like the third strand, it is concerned with same-season production, but it differs in three respects. First, rather than forecasting production from mean weather conditions, it measures the realized consequences of an extreme event. This is precisely the type of episode that Santos et al. (2020) note their model does not capture. Second, rather than improving measurement at the level of individual vineyards, it borrows strength across units, allowing reliable estimates to be produced for cells that were sparsely sampled or not sampled at all. And third, it can be applied during the dormant season: after a cold event has already set an upper bound on production, but months before vineyard-level yield estimation methods are typically deployed. Relative to the fourth strand, it builds directly on bud mortality surveys. It replaces survey disaggregation with a model-based approach that extends their coverage, reduces sampling error in sparsely sampled cells, and translates bud mortality into production losses at the region, variety, and industry levels. This includes estimates of the kind that may have enabled more timely intervention in the New York case.

Three further connections are worth noting. First, our methodology addresses both limitations identified by Puga and Anderson (2025a, 2025b). Multi-level modelling permits heterogeneous estimates across region-variety cells from sparse data, while identification from cross-sectional variation within a single event removes the need for a long history of comparable extremes. Second, it complements rather than competes with cold hardiness models. Those models anticipate risk before a cold event, informing real-time on-farm mitigation such as the deployment of frost protection. Our methodology measures realized damage after the event, informing the market- and policy-based interventions that follow. Third, we highlight that our proposal brings small area estimation back to its agricultural roots.

Battese et al. (1988) introduced the nested-error regression model to predict county-level corn and soybean areas in Iowa, where farm survey data were too sparse to support direct estimates, by combining survey observations with satellite data. Model-based small area estimation has since been recommended for, and developed within, the official county-level crop estimates of the US Department of Agriculture (Erciulescu et al. (2019)).

3. Methodological Proposal

3.1. **Procedure.** Our proposed methodology for measuring grapevine cold injury and production losses consists of four steps. In the first step, a generalized linear mixed model (Breslow and Clayton (1993)) is used to estimate the relationship between variety- and region-level covariates and the probability that bud sample i of variety v in region r had a positive bud mortality status ($Pr(m_{i,r[i],v[i]} = 1)$). This model takes the following general form:

$$Pr(m_{i,r[i],v[i]} = 1) = logit^{-1}(\alpha + \boldsymbol{x}_{i,r[i],v[i]}\beta + \alpha_{r[i]} + \alpha_{v[i]}) \quad \text{for} \quad i = 1, ..., N \tag{2}$$

where

$$\alpha_r \sim N(0, \sigma_r^2) \quad \text{for} \quad r = 1, ..., R \tag{3}$$

$$\alpha_v \sim N(0, \sigma_v^2) \quad \text{for} \quad v = 1, ..., V \tag{4}$$

Each variable is indexed over individual bud sample i and the hierarchical levels to which those bud samples can be grouped into; namely, region r and variety v. α is a fixed intercept; $\boldsymbol{x}_{r[i],v[i]}$ is a vector consisting of covariates that describe the cold exposure faced by bud sample i of variety v in region r, its state of acclimation, and their interactions[7]; and β is a vector of fixed regression coefficients conformable with $\boldsymbol{x}_{r[i],v[i]}$. By contrast, $\alpha_{r[i]}$ and $\alpha_{v[i]}$ are region- and variety-level random effects. These terms serve as intercept offsets that capture unobserved between-group heterogeneity. The random effects for grouping factors r and v are modelled as being drawn from normal distributions with mean zero and variances σ_r^2 and σ_v^2, respectively. The result of this specification is partial pooling: grouping factors with few samples, high residual variance, and small between-group variance shrink toward the grand mean (thus borrowing strength from other cells) whereas those with many samples, low residual variance, and large between-group variance pull away from the grand mean (Gelman and Hill (2007), Lax and Phillips (2009)). Generalized linear mixed models are estimated via (approximate) marginal maximum likelihood and can be implemented, for instance, using the *glmer*() function in R's *lme*4 package (Bates et al. (2003)). Because primary and secondary buds differ in their susceptibility to cold injury (Fennell (2004),

[7]Refer to Sections 3.2 and 4.1 for further discussion on covariate selection.

Keller (2020)) and both contribute to the productive capacity of a grapevine (Wolfe (2001)), equations (2)-(4) are estimated separately for samples of primary and secondary buds. We note that this does not impose any additional burden on data collection, as primary and secondary buds are collected and logged simultaneously due to their paired nature within the compound bud.

In the second step, the fitted models of primary and secondary bud mortality are used to project the primary and secondary bud mortality rates of each cell in the population. In a wine region with R sub-regions and V varieties planted, there are at most $(R \times V)$ cells, since all varieties may not be planted in all regions. These cells can be viewed as distinct bud types, each with a unique probability of succumbing to cold injury due to differences in their cold exposure (varying in the region dimension) and acclimation state (varying in both the region and variety dimensions). We denote these cell-level projections of the primary and secondary bud mortality rate by $\hat{m}^p_{r,v}$ and $\hat{m}^s_{r,v}$, respectively.

In the third step, we convert the paired bud mortality rate projections of each cell into potential yield. As discussed in Section 2.1, potential yield is a function of the primary and secondary bud mortality rates and can be interpreted as an upper bound on a grapevine's (or, by means of aggregation, a cell's) productive capacity as it enters the growing season. This transformation is as follows:

$$\hat{y}^*_{r,v} = max\ \{1,\ (1 - \hat{m}^p_{r,v}) + 0.25(1 - \hat{m}^s_{r,v})\} \tag{5}$$

And in the fourth step, the cell-level potential yield estimates $\hat{y}^*_{r,v}$ are post-stratified to produce estimates of potential yield at alternative hierarchical levels, including regions, varieties, or the industry at large. Post-stratification weights $(w_{r,v})$ are based on the counterfactual production capacity of the cells had no bud mortality occurred, which can be inferred from recent crop censuses[8]. This approach corrects for imbalances between the distribution of bud samples across cells and the contributions of cells to aggregate production capacity within each grouping factor. Post-stratified estimates of potential yield at the region $(\hat{y}^*_r)$, variety $(\hat{y}^*_v)$, and industry $(\hat{y}^*)$ levels are thus computed as follows:

$$\hat{y}^*_r = \frac{\sum_{v \in V} w_{r,v} \hat{y}^*_{r,v}}{\sum_{v \in V} w_{r,v}} \quad \text{for} \quad r = 1, ..., R \tag{6}$$

[8]Refer to Section 3.2 for further discussion of counterfactual production capacity.

$$\hat{y}^*_v = \frac{\sum_{r \in R} w_{r,v} \hat{y}^*_{r,v}}{\sum_{r \in R} w_{r,v}} \quad \text{for} \quad v = 1, ..., V \tag{7}$$

$$\hat{y}^* = \frac{\sum_{r \in R} \sum_{v \in V} w_{r,v} \hat{y}^*_{r,v}}{\sum_{r \in R} \sum_{v \in V} w_{r,v}} \tag{8}$$

3.2. **Data Requirements.** The data requirements of this procedure can be separated into three components. Together, these components determine the extent to which practitioners are able estimate a well-specified mortality model, achieve broad modelling coverage across cells, and post-stratify cell estimates to alternative hierarchical levels.

3.2.1. *Access to a Bud Mortality Survey.* First and foremost, the procedure requires access to a bud mortality survey. Bud samples should be collected and examined in line with best practice guidelines such as those published by the Cool Climate Oenology and Viticulture Institute at Brock University (Willwerth et al. (2014)). Additionally, each bud sample must be tagged according to their location[9], grape variety, time of collection,[10] and type.[11] Such surveys are routinely conducted in cool-climate wine regions by local research institutions and commercial wineries, meaning that this data requirement does not impose any additional burden on data collection. Surveys from multiple entities may need to be aggregated to ensure sufficient sample sizes and maximize geographic and varietal coverage.

3.2.2. *Access to Covariates.* Second, the procedure requires auxiliary data that explain cross-sectional variation in bud mortality. As discussed in Section 2.2, bud mortality is driven not only by the severity of cold exposure faced by a grapevine, but also by its acclimation state. However, while various exposure-based metrics can easily be computed from high-frequency (hourly) temperature data during the cold event[12], the acclimation state of a grapevine is much more difficult to observe directly. Lethal temperature exotherms are the most reliable measure of cold hardiness, identifying the temperature at which a selected percentage of buds were observed to have frozen. However, such data are rarely available beyond a small

[9]Location is typically recorded based on the sub-region the sample was collected from. However, nothing would prevent samples from being modelled at the vineyard level should sufficient data be available.

[10]Accurately recording the time of collection ensures that appropriate temporal cutoffs can be applied during the construction of various measures of cold exposure.

[11]As discussed in Sections 2.1 and 2.2, primary and secondary buds differ in their susceptibility to cold injury and should therefore be modelled independently. The estimation of mortality models for both bud types is also necessary for the calculation of potential yield (Wolfe (2001)).

[12]For instance, in line with evidence from Chang et al. (2024), one could capture both the depth and duration of exposure by identifying the minimum temperature observed prior to sample collection and computing the duration of exposure below a selected temperature threshold.

selection of cells that are monitored continuously throughout the dormant season. In their absence, we propose that acclimation state proxies be introduced into model specifications as interaction terms. These interaction terms modify the sensitivity of observational units to exposure-based covariates according to observable predictors of cold hardiness. Four such predictors – chill accumulation, grape variety, vine age, and vine health status – were introduced in Section 2.2, but these are not exhaustive. Vineyard management practices such as crop load, irrigation, and nutrient management can also influence a grapevine's acclimation state (Howell (1988), Wample and Wolf (1997)). Meanwhile, site characteristics such as elevation and cold air drainage, together with on-farm mitigation strategies such as wind machines, geotextiles, and vine burial, can cause the cold exposure a grapevine actually experiences to differ from that recorded in regional temperature data (Zabadal et al. (2007), Willwerth et al. (2014)). Where data on such factors are available, they can be incorporated as additional covariates or interaction terms. Where they are not, their influence is partly absorbed by the region- and variety-level random effects described in Section 3.1.

We also note that when applying this procedure, there may at times be a trade-off between model complexity and modelling coverage. This is because the availability of covariates across cells determines the number of cells our proposed methodology is able to produce bud mortality estimates for. Thus, while it may be desirable to specify a more complex first-stage model (for example, by incorporating a broad set of acclimation state variables), doing so may come at the expense of producing estimates for all cells in the population. This is likely to be a practical concern in wine regions for which surveys of vine age or disease prevalence were only conducted across a subset of regions. To shed light on how complex a first-stage model is required to deliver reasonable predictive performance, we thus examine the predictive performance of first-stage model specifications with more limited covariates in Section 4.4.

3.2.3. *Access to Post-Stratification Weights.* Finally, weights are required to post-stratify cell estimates to alternative hierarchical levels. Because the outcome being post-stratified is potential yield, the weights should reflect each cell's contribution to aggregate production capacity: that is, the volume each cell would have produced had no bud mortality occurred. We refer to this quantity as counterfactual production capacity. It depends not only on the crop area within each cell, but also on its target crop load (production per unit area), which may vary across regions and grape varieties (Dobrei et al. (2016), Merot et al. (2022), Puga and Anderson (2024)). How it is best estimated depends on the crop census data available.

Counterfactual production capacity can be estimated most reliably in wine regions that report both crop area and production on an annual basis[13]. In these settings, it can be

[13]This is the case, for example, for crop censuses conducted by the US Department of Agriculture (California) and the University of Oregon (Oregon).

approximated as the product of each cell's current crop area and its target crop load. Crop area can be sourced directly from the most recent crop census. Target crop load, by contrast, must be approximated from multiple vintages, since the crop load realized in any given year also reflects that year's growing conditions. We propose approximating it by the maximum crop load observed within each cell across the H most recent crop censuses. This choice reflects an asymmetry in crop load management (Howell (2001)). When favourable conditions put upward pressure on crop load, vineyard operators can readily reduce it through pruning and crop thinning, but they lack what Howell (2001) calls "lower control" when adverse conditions push crop load below its target. Realized crop loads therefore rarely exceed their target by much, but often fall short of it in adverse years, so the maximum across recent vintages provides the closest approximation. The choice of H involves a trade-off. A longer horizon increases the probability that each region experienced at least one vintage with growing conditions conducive to achieving its target crop load, but it also increases the probability that target crop loads changed during the reference period.

This approach is less reliable in wine regions where up-to-date data on crop area are unavailable. This is common, as many wine regions conduct production-based censuses annually but survey crop area only periodically[14]. Because crop area may have changed since the most recent area survey, counterfactual production capacity may be more reliably estimated from historical production alone. By the same logic as above, we propose approximating it by the maximum production volume observed within each cell across the H most recent crop censuses. The choice of H involves the same trade-off, with one addition: longer horizons also increase the probability that crop areas changed meaningfully during the reference period. In either setting, a practical guide is to ask: "What is the shortest horizon for which all modelled regions experienced growing conditions conducive to achieving their target crop load?"

4. Empirical Application

On December 18^{th}, 2022, temperatures declined rapidly across many parts of British Columbia. Temperatures dropped by as much as $20°C$ within a 24-hour period, exposing 13 of the province's wine-producing regions to temperatures below -$20°C$ (see Figure 1). Some regions remained below this threshold for up to 102 hours and some experienced temperatures below -$30°C$. With approximately 9 months until harvest, there was thus significant interest in understanding the magnitude and distribution of grapevine cold injury and production losses across the 401 exposed cells. However, given the resource-intensive nature of collecting and analysing bud samples, the primary and secondary bud mortality rates of many cells were either unobserved (due to zero sample sizes) or unreliable (due to

[14]This is the case, for example, for the BC Wine Grape Council's Crop Assessment (annual; production-based) and Acreage Report (periodic; area-based).

small sample sizes). In this section, we apply our proposed methodology to a bud mortality survey conducted shortly after this cold event to demonstrate how it could have helped address these informational gaps in real time.

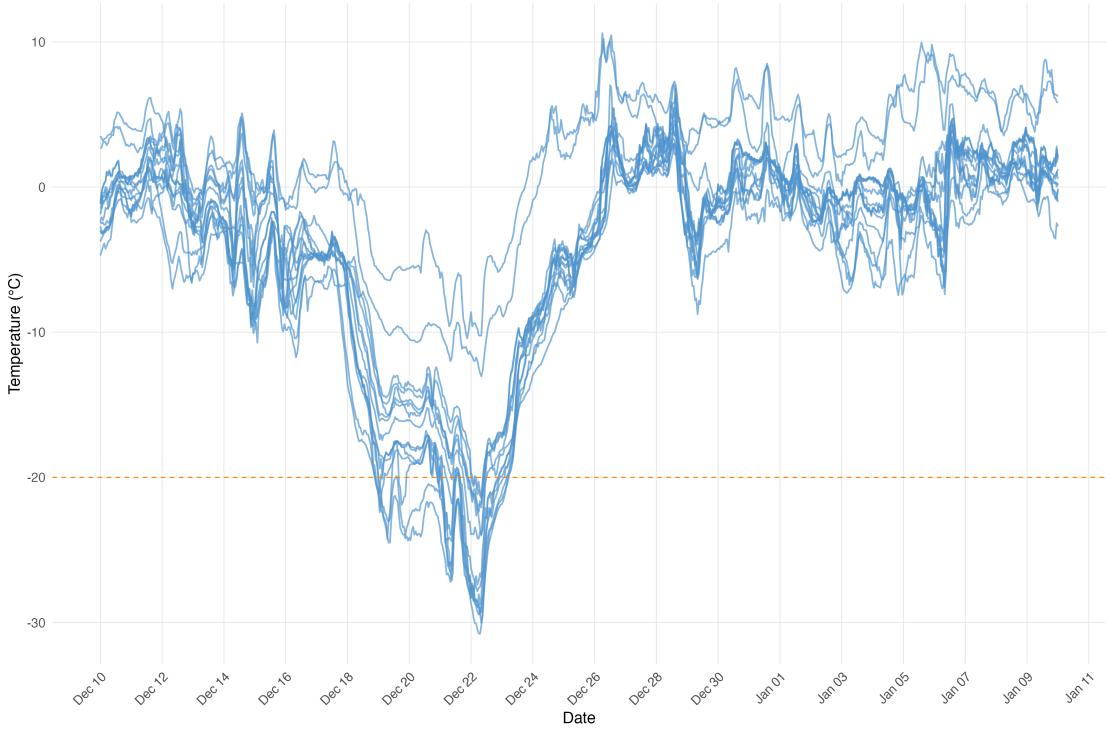


Figure 1. Hourly minimum temperatures observed across the British Columbia's wine-producing regions between December 10^{th}, 2022 and January 10^{th}, 2023. -20°C reference line is included in orange.

4.1. **Materials & Methods.**

4.1.1. *Bud Mortality Survey.* We obtain access to 20,651 primary bud samples and 20,649 secondary bud samples collected in January 2023 by the Summerland Research and Development Centre[15] and 39 commercial vineyards.[16] The distribution of bud samples across cells (Table 1) illustrates the shortcomings of the survey disaggregation method in this setting. First, zero samples were collected from 346 cells, meaning that estimates of the primary and secondary bud mortality rates could not be produced via survey disaggregation for the majority (86.3%) of cells. These unsampled cells account for 29.4% of total counterfactual

[15]The Summerland Research and Development Centre is operated by Agriculture and Agri-Food Canada, a department of the federal government of Canada.
[16]These vineyards requested that they remain anonymous.

production capacity.[17] Second, of the 55 cells that were sampled, many had insufficient sample sizes to produce reliable estimates via the survey disaggregation method. Depending on the degree of sampling error deemed acceptable, reliable estimates could only be produced for 3.2–6.4% of cells, equivalent to 46.1–53.7% of total counterfactual production capacity. Our proposed methodology aims to increase the number of cells for which reliable estimates can be computed from the same underlying bud mortality survey.

Table 1. Distribution of primary and secondary bud samples across cells

	Primary Buds	**Secondary Buds**
No. of samples	20,651	20,649
No. (%) of regions sampled	7 (53.8%)	7 (53.8%)
No. (%) of varieties sampled	24 (26.1%)	24 (26.1%)
No. (%) of cells sampled	55 (13.7%)	55 (13.7%)
No. (%) of unsampled cells	346 (86.3%)	346 (86.3%)
No. (%) of cells with 1-49 samples	15 (3.7%)	15 (3.7%)
No. (%) of cells with 50-99 samples	14 (3.5%)	14 (3.5%)
No. (%) of cells with 100-249 samples	7 (1.7%)	7 (1.7%)
No. (%) of cells with 250-499 samples	6 (1.5%)	6 (1.5%)
No. (%) of cells with 500+ samples	13 (3.2%)	13 (3.2%)
Production share* of unsampled cells	29.4%	29.4%
Production share* of cells with 1-49 samples	6.0%	6.0%
Production share* of cells with 50-99 samples	11.0%	11.0%
Production share* of cells with 100-249 samples	3.4%	3.4%
Production share* of cells with 250-499 samples	4.2%	4.2%
Production share* of cells with 500+ samples	46.1%	46.1%

* Production share is based on counterfactual production capacity (see Section 4.1.4)

4.1.2. *Exposure Covariates.* To measure cold exposure across regions, we access hourly temperature data for 78 weather stations in southern British Columbia from the NOAA's Global Historical Climatology Network - Hourly (GHCN-h) database (Menne et al. (2023)). Because missing observations could bias measures of cold exposure, we record the number of missing observations for each weather station during the 2023 vintage's dormant season, omit those missing more than 5% of observations over this period, and impute any missing values for the retained stations.[18] 54 weather stations were retained after this procedure. Hourly temperature observations were then mapped from weather stations to British Columbia's

[17] See Section 4.1.4 for more information on how counterfactual production capacity is computed.

[18] Missing observations for stations exceeding the minimum completeness criterion are filled by linear interpolation using the *na.approx()* function in the *zoo* package in R.

wine-producing regions using the point-to-polygon spatial transformation outlined in Appendix B.1. We denote the hourly temperature observation in region r at time t by $T_{r,t}$.

For our primary first-stage model specification, we compute a cumulative measure of cold exposure below a fixed temperature threshold $\bar{T}$. This bespoke measure, which we refer to as the freeze severity index, aligns with experimental evidence by Chang et al. (2024) which finds that bud mortality is influenced by both the depth and duration of cold exposure. It is also conceptually similar to growing degree days, a cumulative measure of heat exposure during the growing season that is widely used in agriculture to monitor plant development (McMaster and Wilhelm (1997)). The freeze severity index for region r (FSI_r) is computed as follows:

$$FSI_r = \sum_{t \in S} max(0, \bar{T} - T_{r,t}) \tag{9}$$

where S is the set of hourly observations spanning the beginning of the dormant season (November 1, 2022) through to sample collection (January 10-13, 2023). Exposure covariates are then mapped to individual bud samples based on the region in which they were collected. A larger value of FSI_r can be interpreted as a more severe cold exposure. The fixed temperature threshold is set at -20°C in our primary first-stage model specification, with two alternative thresholds (-15°C, -17.5°C, -22.5°C, and -25°) explored for robustness in Section 4.4. Summary statistics are provided in Table A.1.

For robustness, we also compute the depth and duration of cold exposure as separate covariates. We define the depth of exposure ($depth_r$) as the absolute minimum temperature observed in region r between the beginning of the dormant season and when the bud mortality surveys were conducted. Duration of exposure ($duration_r$) is defined as the total number of hours for which $T_{r,t}$ falls below a fixed exposure threshold of -20°C over the same horizon. The out-of-sample performance of a first-stage model specification with these alternative exposure covariates is evaluated in Section 4.4. Bud samples again adopt the exposure covariates from the region in which they were collected.

4.1.3. *State Covariates.* In this empirical application, we utilize four separate covariates that proxy for a grapevine's acclimation state. First, we compute chill accumulation across regions by applying the chilling hours model (Weinberger (1950)) to the hourly temperature data described in Section 4.1.2. This model defines chill accumulation as the total number of hours for which observed temperatures were between 0°C and 7.2°C. We compute this covariate at the region level (denoted by $chill_r$) based on temperature observations spanning the beginning of the dormant season through to the cold event (December 18th, 2022). $chill_r$ is then mapped to individual bud samples based on the region in which the samples were collected. For robustness, we also evaluate the out-of-sample performance of a model

specification that utilizes an alternative model of chill accumulation – the Utah chill model (Richardson et al. (1974)) – in Section 4.4.

Second, to account for varietal differences in cold susceptibility, we utilize the frost ratings (denoted by $susceptibility_v$) published by VineTech Canada (2025). VineTech Canada is one of the country's leading domestic nurseries, providing Canadian vineyards with access to both domestically grown and imported grapevines for more than 22 years. These frost ratings, which range from 1 (least susceptible) to 10 (most susceptible), are one of several product characteristics provided across their catalogue of grape varieties. However, frost ratings are only available for 35 out of the 92 grape varieties actively cultivated across the 13 affected wine regions in British Columbia. The impact of this data gap on our ability to produce bud mortality estimates across the 401 cells in this empirical application is discussed in Section 4.2.1. Similar to covariates that were mapped to bud samples based on the region in which they were collected, $susceptibility_v$ is mapped to individual bud samples based on the samples' grape variety. See Table A.2 for a list of varieties and their frost ratings.

Third, we access data on vine age from an industry report commissioned by the British Columbia Ministry of Agriculture and Food and completed by Terroir Consulting (Esau et al. (2024)). Because newly planted grapevines are more susceptible to cold injury, we focus on the percentage of plantings within each region that were 3 years old or less in 2023. We denote this covariate by age_r, noting that it is mapped to individual bud samples based on the region in which they were collected. Summary statistics are provided in Table A.1, with age_r ranging from 0.0% to 22.4%.

And fourth, to account for the impact of adverse health conditions on grapevine cold hardiness, we access data on the prevalence of grapevine virus and disease across British Columbia's wine-producing regions from Urbez-Torres (2016). $disease_r$ denotes the percentage of sampled vineyard blocks within region r that tested positive for grapevine leafroll-associated viruses (GLRaVs). While more timely data on grapevine virus and disease prevalence would be preferable, it is our understanding that more recent survey data is not available. $disease_r$ varies significantly across regions, ranging from 12.0% in the Similkameen Valley to 67.0% in Oliver and Osoyoos. Additional summary statistics are provided in Table A.1. Similar to other covariates, $disease_r$ is mapped to individual bud samples based on the region in which they were collected.

4.1.4. *Post-Stratification Weights.* To compute post-stratification weights, we access historical production data from the British Columbia Wine Grape Council (2025) (the 'Council') to compute the counterfactual production capacity of each cell had zero bud mortality been observed. Production volumes, broken down by region and grape variety, are collected annually by the Council to facilitate the calculation of a mandatory volumetric levy established under the Farming and Fishing Industries Development Act of 2006. Because this is a mandatory

reporting requirement for all vineyards in British Columbia, the published data provides a solid basis for computing counterfactual production capacity. As discussed in Section 4.1.4, we approximate a cell's counterfactual based on the maximum annual production volume observed within that cell over the preceding H years. Given the 2022 vintage produced a record harvest of 42,732.2 tons, we set a relatively short horizon of $H = 3$ in this empirical application. This choice balances the tension between maximizing the probability that each cell will have (approximately) achieved its target crop load (increasing in H) and minimizing the probability that unobserved structural changes – such as non-trivial changes to crop area or target crop loads – will have occurred (also increasing in H). Counterfactual production capacity varies significantly across cells, ranging from as low as 1 ton to as high as 4,755 tons. Additional summary statistics can be found in Table A.1.

4.1.5. *First-Stage Model Specifications.* To produce the bud mortality and potential yield estimates reported in Section 4.2, we estimate the following generalized linear mixed model by (approximate) marginal maximum likelihood (Breslow and Clayton (1993)):

$$\begin{aligned} Pr(m_{i,r[i],v[i]}) = \; & logit^{-1}(\alpha + \alpha_{r[i]} + \alpha_{v[i]} + \beta_1 FSI_{r[i]} + \\ & \beta_2(FSI_{r[i]} \times chill_{r[i]} \times susceptibility_{v[i]}) + \\ & \beta_3(FSI_{r[i]} \times chill_{r[i]} \times susceptibility_{v[i]} \times age_{r[i]}) + \\ & \beta_4(FSI_{r[i]} \times chill_{r[i]} \times susceptibility_{v[i]} \times disease_{r[i]}) + \\ & \beta_5(FSI_{r[i]} \times chill_{r[i]} \times susceptibility_{v[i]} \times age_{r[i]} \times disease_{r[i]})) \\ & \text{for} \quad i = 1, ..., N \end{aligned} \tag{10}$$

where

$$\alpha_r \sim N(0, \sigma_r^2) \quad \text{for} \quad r = 1, ..., R \tag{11}$$

$$\alpha_v \sim N(0, \sigma_v^2) \quad \text{for} \quad v = 1, ..., V \tag{12}$$

As discussed in Section 3.2.2, this specification can be understood as a (state × exposure) interaction model. The probability of a bud sample i of variety v in region r succumbing to cold injury is increasing in cold exposure (FSI_r), but the marginal effect is allowed to vary across cells based on regional and varietal differences in grapevine cold acclimation (proxied by $chill_r$, $susceptibility_v$, age_r, and $disease_r$). Region and variety random effects (α_r and α_v, respectively) serve to soak up additional between-group heterogeneity, which could include unobserved differences in cold exposure or acclimation.[19]

[19]Unobserved differences in cold exposure could be driven, for example, by regional differences in the adoption of cold mitigation strategies such as wind machines, geotextiles, or vine burial. However, these strategies are highly capital- and resource-intensive and are therefore not widely adopted in British Columbia (Esau et al. (2024)).

For robustness, we also evaluate the out-of-sample performance of several alternative first-stage model specifications in Section 4.4. First, to better understand which terms in equation (10) are driving the model's predictive performance, we consider a series of nested specifications. Second, to evaluate the sensitivity of our model's predictive performance to the selection of the fixed temperature threshold $\bar{T}$ used in the computation of FSI_r, we consider specifications in which FSI_r is computed based on thresholds of $-15°C$, $-17.5°C$, $-22.5°C$ and $-25°C$. Third, we consider alternative state and exposure covariates where they are available. This includes separate measures of the depth and duration of exposure ($depth_r$ and $duration_r$, respectively), as well as an alternative chill model ($utah_r$). These alternative model specifications are listed in more detail in Appendix B.2.

We also consider alternative generalized linear mixed model specifications that supplement specifications A5-A7 with random slope coefficients in the region dimension. The purpose of these specifications is to evaluate whether random slopes – which serve as group-specific slope offsets that are modelled as being drawn from a normal distribution with mean zero and variance Σ_r – can partially make up for limited access to acclimation state covariates. This type of model specification may be valuable, for example, in wine regions for which data on vine age and/or disease prevalence are unavailable. This model takes the following general form:

$$\begin{aligned} Pr(m_{i,r[i],v[i]} = 1) = \; & logit^{-1}(\alpha + \alpha_{r[i]} + \alpha_{v[i]} + \boldsymbol{x}_{r[i],v[i]}\beta + \boldsymbol{x}_{r[i],v[i]}\beta_{r[i]}) \\ & \text{for} \quad i = 1, ..., N \end{aligned} \tag{13}$$

where

$$\alpha_r \sim N(0, \sigma_r^2) \quad \text{for} \quad r = 1, ..., R \tag{14}$$

$$\alpha_v \sim N(0, \sigma_v^2) \quad \text{for} \quad v = 1, ..., V \tag{15}$$

$$\beta_r \sim N(0, \Sigma_r) \quad \text{for} \quad r = 1, ..., R \tag{16}$$

4.2. **Results.**

4.2.1. *Modelling Coverage.* As noted in Section 4.1.3, data on varietal susceptibility to cold injury could only be sourced for 35 out of 92 grape varieties in this empirical application. This data gap constrained the number of cells for which estimates of the primary and secondary bud mortality rates could be produced, with a total of a 168 unmodelled cells. While this is a large proportion of the 401 cells (41.9%), it is nonetheless a substantial improvement relative to the status quo. Under the survey disaggregation method, cell estimates could not be produced for 86.3% of cells and another 7.2% of cells were exposed to substantial sampling error due to limited sample sizes ($n < 100$). When framed in terms of production volumes,

the improvements in modelling coverage from applying our methodology in this setting are even more apparent. While survey disaggregation could only produce reliable estimates[20] for cells accounting for 53.6% of total counterfactual production capacity, our methodology increased this figure to 95.3%, thus providing a near comprehensive view of aggregate grape and wine production losses following the December 2022 cold event in British Columbia.

4.2.2. *Bud Mortality Estimates.* Estimates of the primary and secondary bud mortality rates across cells are visualized in Figures 2 and 3, respectively. Based on these estimates, there was significant variation in grapevine cold injury both within and across regions after the December 2022 cold event. Within-region variation – which exceeded 75 percentage points across cells for the primary bud mortality rates within regions like Summerland-Peachland and Kootenay – is attributable primarily to varietal differences in cold hardiness. The estimated bud mortality rates of cold hardy varieties (such as Pinot Noir and Riesling) are notably lower than those of more cold susceptible varieties (such as Syrah and Merlot) in the same region. For example: In Osoyoos, the primary bud mortality rate of Pinot Noir was estimated to be just 27.3% while that of Syrah was 92.8%. Examples such as this highlight the important role of variety composition in determining the aggregate bud mortality rate within a region. This methodology – which enables more comprehensive evaluations of grapevine cold injury than could be produced via survey disaggregation – may therefore be an important strategic planning tool for regions seeking to mitigate cold injury in the future.

Variation across regions is similarly pronounced. The estimated bud mortality rates are highest in regions which experienced more severe cold exposure (including two of the northernmost regions: Thompson Valley and Lillooet), as well as in regions with more moderate cold exposure but for which our acclimation state proxy variables indicate a lower cold tolerance (such as Oliver, where cold susceptible varieties such as Merlot and Syrah are heavily planted and grapevine virus and disease is understood to be most prevalent). On the low-

[20]It is assumed here that a minimum threshold of 100 samples is required to produce estimates with sufficiently small sampling error to be practically useful for industry stakeholders.

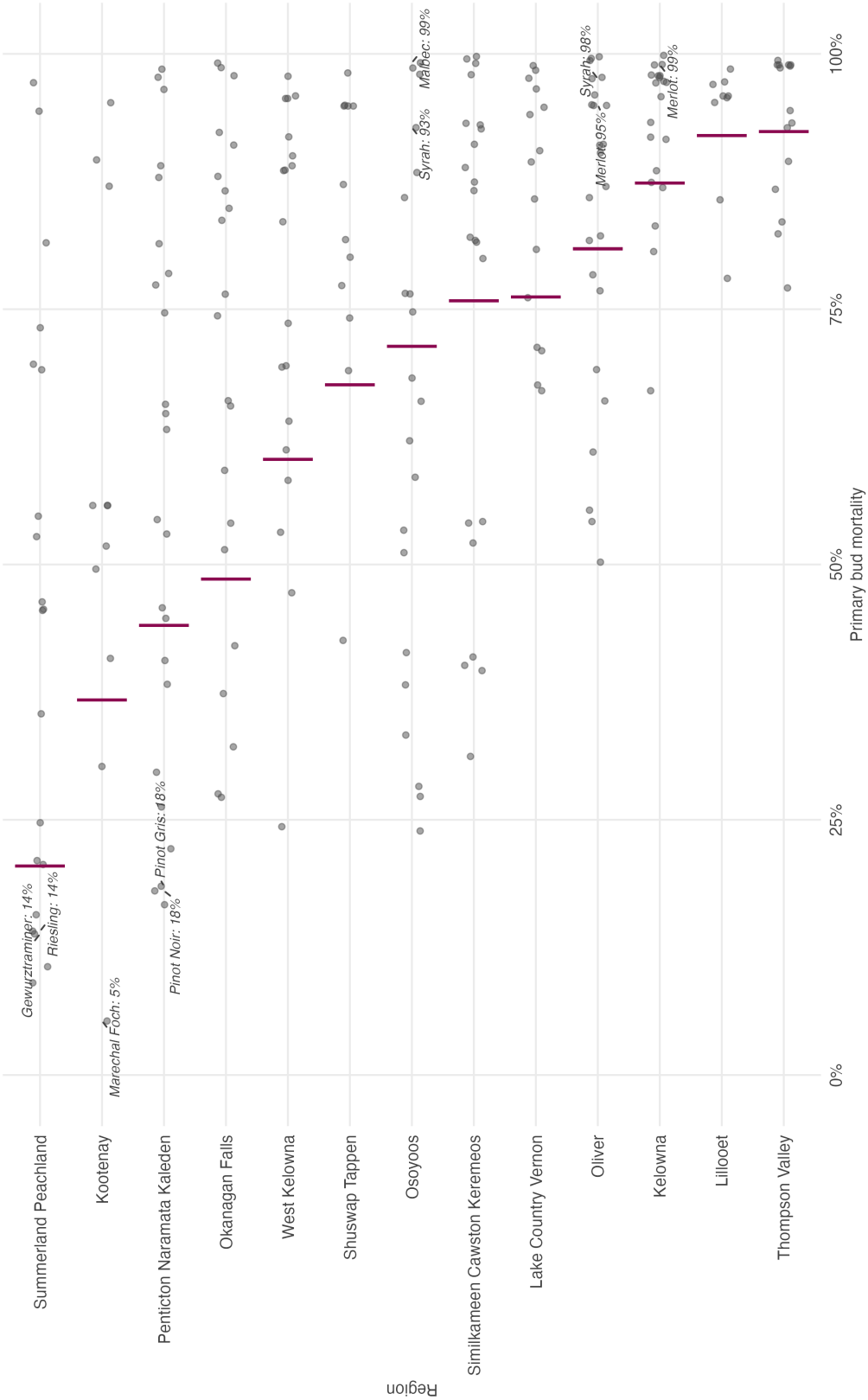


Figure 2. Model-based estimates of primary bud mortality at cell-level. Cell estimates grouped by region to aid interpretation. Red lines indicate the production-based weighted average bud mortality rate within each region.

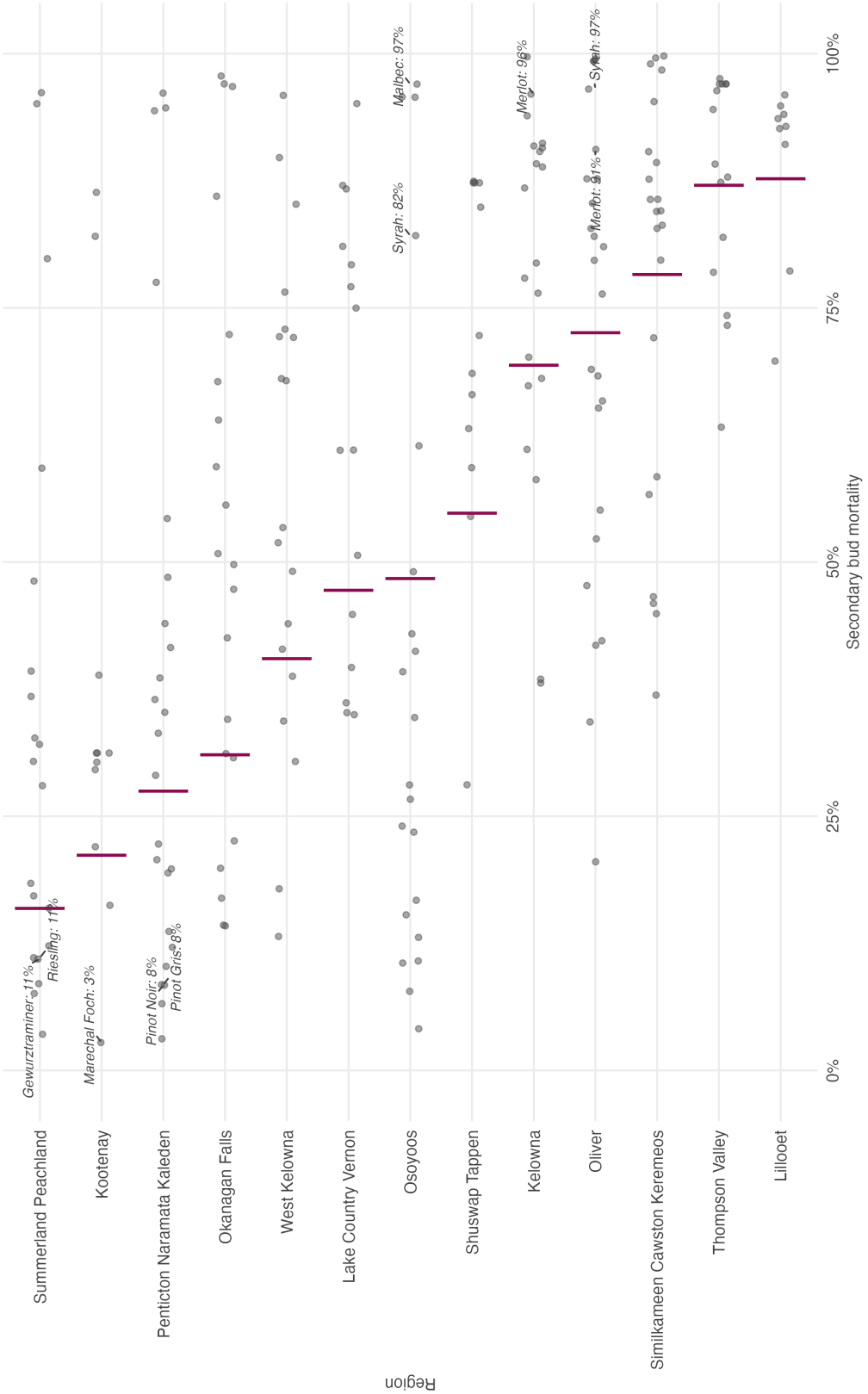


Figure 3. Model-based estimates of secondary bud mortality at cell-level. Cell estimates grouped by region to aid interpretation. Red lines indicate the production-based weighted average bud mortality rate within each region.

-er end of the spectrum are regions like Summerland-Peachland and Penticton-Naramata-Kaleden. While these regions experienced below-average cold exposure, they are also relatively more concentrated in cold hardy varieties than other regions. For instance: Gewurztraminer, Pinot Blanc, Pinot Gris, Pinot Noir, and Riesling (five relatively cold hardy varieties) account for 69.2% of counterfactual production capacity in Summerland-Peachland, but only 32.3% of the counterfactual production capacity of the industry-at-large. This figure also sits well above the industry average in Penticton-Naramata-Kaleden at 45.1%.

Finally, of more tangential interest, Figures 2 and 3 reinforce long-standing evidence that primary buds are more susceptible to cold injury than secondary buds (Keller (2020), Fennell (2004)). Of the 233 cells for which our methodology is able to produce primary and secondary bud mortality estimates, 216 (or 92.7%) observe a higher primary bud mortality rate than secondary bud mortality rate. The mean difference between the primary and secondary bud mortality rates was 14.3 percentage points across cells.

4.2.3. *Potential Yield Estimates.* Post-stratified estimates of potential yield at the region, variety, and industry levels are reported in Figure 4. At the industry level, potential yield was estimated to be just 39.4%. In other words, the negative supply shock associated with the December 2022 cold event in British Columbia was equivalent to 60.6% of grape and wine production volumes. These losses, however, were not distributed equally across regions or grape varieties in our model. Regional differences mirror those discussed in Section 4.2.2 and span more than 82.2 percentage points. Regions with less severe cold exposures and greater concentrations in cold hardy varieties (such as Summerland-Peachland or Penticton-Naramata-Kaleden) were estimated to have experienced relatively modest supply shocks, whereas those with more severe cold exposures (like Thompson Valley) or for which acclimation state proxy variables indicate a higher degree of cold vulnerability (like Oliver) are estimated to have experienced more severe supply shocks.

Crop losses were similarly variable across varieties, with potential yield ranging from 1.3% (or a near total crop loss) for Malbec to 75.0% for Marechal Foch (a French-American hybrid developed to withstand harsh winters). The relative ordering of varieties is largely as expected, with our post-stratified potential yield estimates generally higher for cold hardy varieties (such as Pinot Noir) and lower for those more susceptible to cold injury (such as Syrah). However, our model-based estimates also suggest that some of the most cold hardy varieties planted in British Columbia experienced some of the most severe cold injury and production losses. These more surprising results are driven by the distribution of these grape varieties across regions. For instance, Concord's low potential yield estimate (1.8%) can be attributed to the fact that it is only grown in Thompson Valley, the region with the second largest cold exposure. From a practical perspective, examples such as this highlight

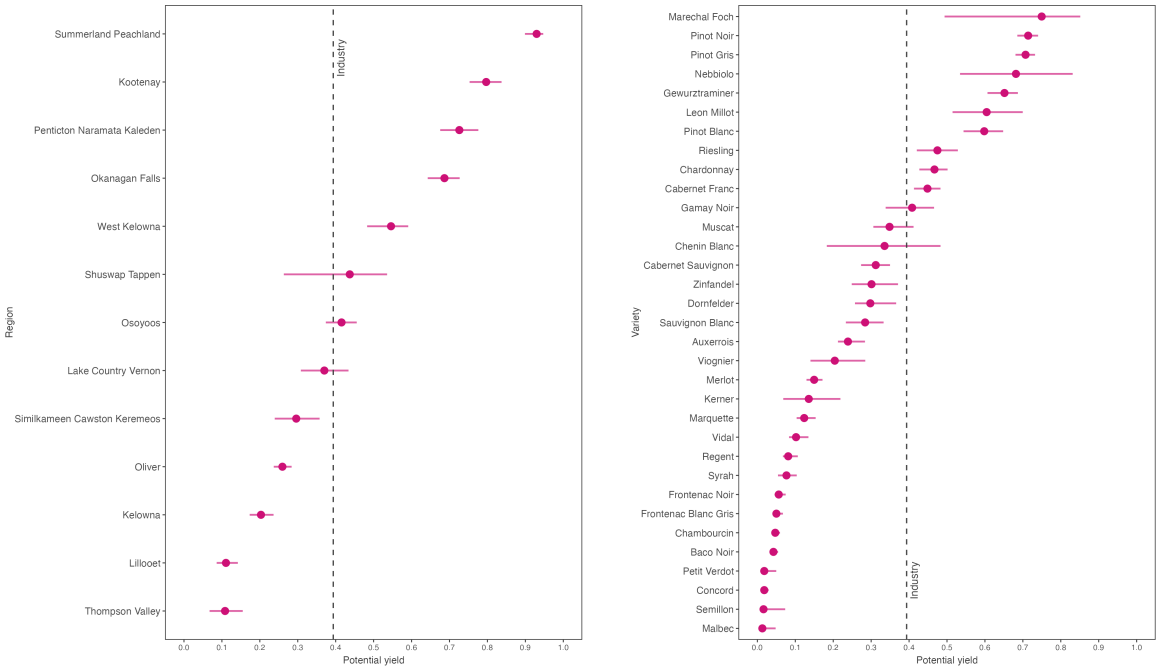


Figure 4. Model-based estimates of potential yield by region (left) and variety (right). Industry estimate is included as a dashed line. Error bars indicate 95% confidence intervals computed using a parametric bootstrap ($R = 1,000$) implemented using the $bootMer()$ function in R's $lme4$ package (Bates et al. (2003)).

the importance of focusing on within-region comparisons when evaluating production losses across varieties for strategic planning purposes.

4.3. **Model Validation.**

4.3.1. *Out-of-Sample Predictive Performance.* The primary benefit of our proposed methodology for measuring grapevine cold injury and production losses is its ability to produce estimates for unsampled cells. However, just because it can do so does not necessarily mean that those estimates are reliable. In this section, we perform leave-one-out cross-validation (LOOCV) to evaluate the out-of-sample performance of our methodology. We do so as follows. First, we identify cells in which there are a sufficient number of samples to produce bud mortality estimates via survey disaggregation that are subject to a relatively small degree of sampling error. We set this threshold at 500 samples, resulting in a validation set of 13 cells that span 3 regions and 9 varieties (see Table A.3 for a complete list of these cells). We treat the estimates computed for these cells via survey disaggregation (which we refer to as direct estimates) as a reliable source of truth that we can evaluate our model-based estimates against. Second, for each cell in the validation set, we omit all bud samples from that cell and re-compute a model-based estimate for that cell using our methodology. The first-stage model specification is again based on equations (10)-(12). This results in a single

out-of-sample prediction for each cell in our validation set. And third, we assess our methodology's out-of-sample predictive performance by computing the mean absolute error (MAE) and root mean squared error (RMSE) between the 13 out-of-sample predictions and their associated direct estimates.

LOOCV results are reported in Figure 5, illustrating the ability of our model to produce reliable estimates of bud mortality for unsampled cells. For the primary bud mortality rate, it achieves a MAE of 4.9 percentage points and a RMSE of 6.2 percentage points. These margins of error are comparable to those achieved in other applications of small area estimation (Lax and Phillips (2009), Buttice and Highton (2013) Howe et al. (2015)), demonstrating the ability of multi-level regression and post-stratification to generalize to novel domains. There are also no major outliers, with the margin of error relatively consistent across cells. We do note, however, that our methodology's performance deteriorates somewhat for secondary buds, achieving a MAE and RMSE of 8.4 and 9.9 percentage points, respectively. The reasons for this deterioration are not well understood at this time, but may be partially attributable to measurement error[21] or differential physiological responses to cold exposure that necessitate a distinct model specification for secondary buds. Nonetheless, the magnitude of these margins of error for the secondary bud mortality rate should not dissuade practitioners from using this methodology in response to future cold events, particularly given the subordinate nature of secondary buds in the computation of production losses.

4.3.2. *Small Sample Performance.* A secondary benefit of our methodology is its ability to produce more reliable estimates for cells in which only a small number of samples were collected. To demonstrate, we perform the small sample validation procedure popularized by Lax and Phillips (2009) and Pacheco (2011). Focusing again on the subset of cells with at least 500 samples, we conduct simulations that utilize a subset of the data to generate both direct estimates (via survey disaggregation) and model-based estimates (via our methodology) of the primary and secondary bud mortality rates in our 13 validation cells. These simulations artificially reduce the number of bud samples within a validation cell to $n_s \in \{10, 25, 50, 100, 200\}$ and compute estimates from these restricted samples. The direct and model-based estimates produced from these restricted samples are then compared to the direct estimate produced from the unrestricted sample.[22] Finally, to conclude the procedure, the MAEs of the restricted estimates are computed relative to the unrestricted estimate across simulations at each value of n_s. 99 simulations are conducted for each value of n_s across each validation cell for both the primary and secondary bud mortality rates, resulting in a total of $(99 \times 5 \times 13 \times 2) = 19,305$ simulations.

[21]Measurement error may be more likely when evaluating the mortality status of secondary buds, which are smaller and can be more difficult to identify in the field.

[22]As in Section 4.3.1, the direct estimates produced from all bud samples within validation cell i is treated as a reliable source of truth given its large sample size.

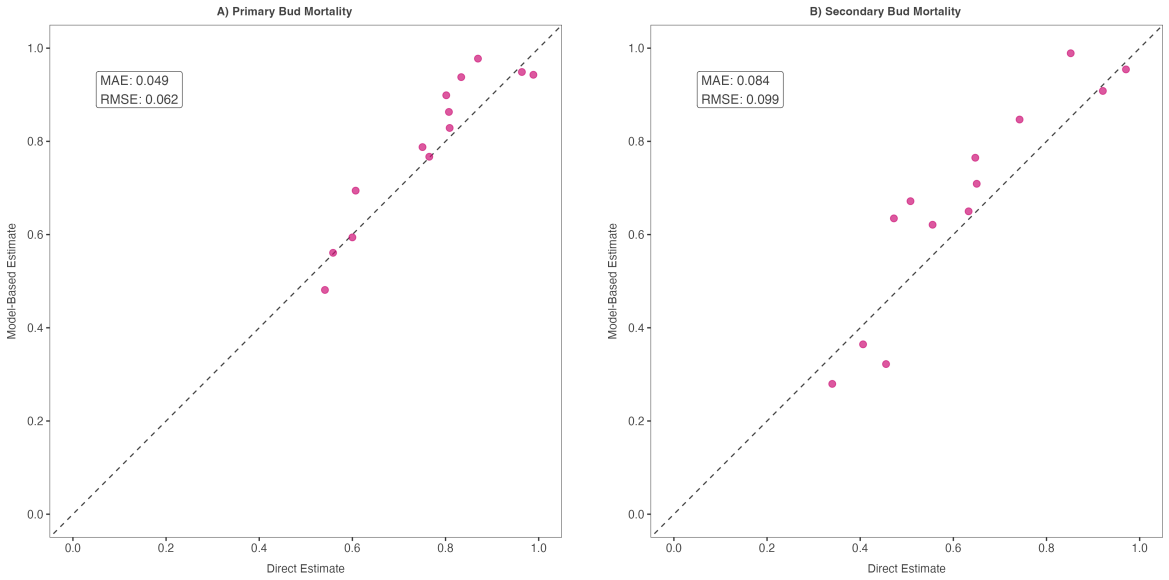


Figure 5. Leave-one-out cross-validation results for the primary (left) and secondary (right) bud mortality rates of heavily sampled cells ($n \geq 500$). MAE and RMSE denote the mean absolute error and root mean squared error, respectively.

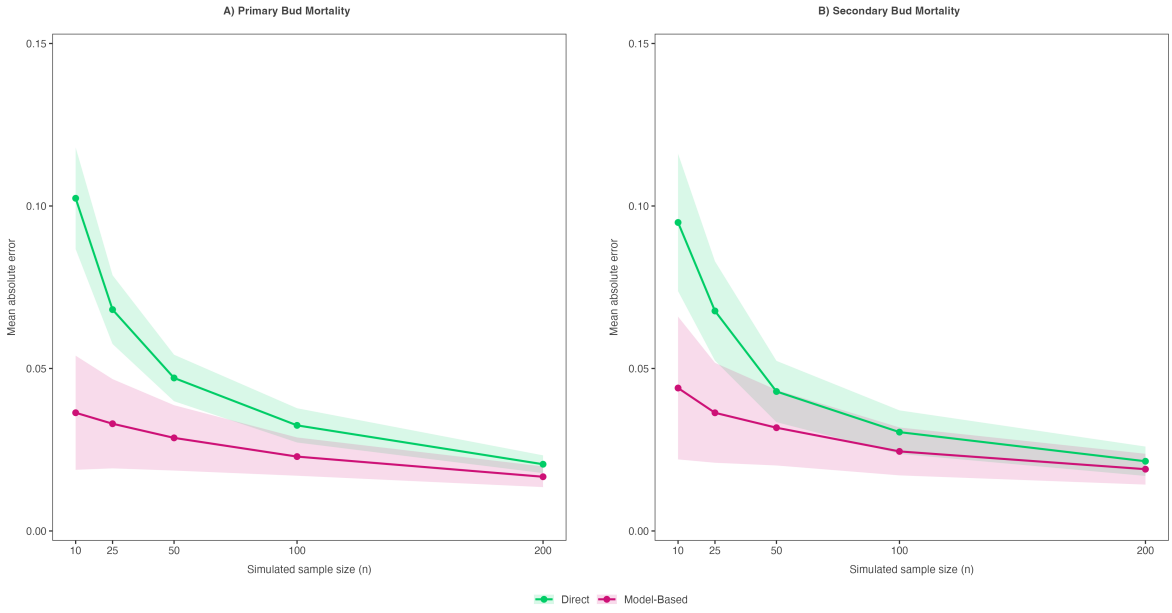


Figure 6. Small sample simulation results for the primary (left) and secondary (right) bud mortality rates of heavily sampled cells ($n \geq 500$). Error bars are computed as two standard deviations of the absolute error across simulations.

Results from these small sample simulations are visualized in Figure 6. Under sufficiently large sample sizes, the MAE of estimates produced using our methodology is approximately equal to (if not slightly lower than) the MAE of estimates produced via survey disaggregation. This means that even in heavily sampled cells, there is not a distinguishable benefit to using direct estimates over those produced by our methodology. However, there is a notable divergence between the two methodologies that occurs below a simulated sample size of 100. By taking a model-based approach that borrows strength across cells, our methodology sees a relatively modest deterioration in its predictive performance as sample sizes shrink. For instance: our methodology achieves a MAE of 2.2 percentage points for the primary bud mortality rate at a simulated sample size of 100, with this value increasing by only 1.4 percentage points (to 3.6 percentage points) as we move to a simulated sample size of 10. By contrast, the MAE of estimates produced via survey disaggregation increased more than three-fold over this same interval, growing from 3.2 percentage points at $n_s = 100$ to 10.2 percentage points at $n_s = 10$. The same general pattern is observed for the secondary bud mortality rate (although the difference is somewhat less pronounced). This gulf in performance in small sample settings further strengthens the case for utilizing our methodology over survey disaggregation in response to future cold events.

4.4. **Performance of Alternative First-Stage Model Specifications.** Finally, to conclude this empirical application, we compare and contrast the performance of our methodology under a series of alternative first-stage model specifications. These comparisons are based on out-of-sample performance (computed via leave-one-out cross-validation as in Section 4.3.1), with the results presented in Table 2.

4.4.1. *Nested Specifications.* Panel A of Figure 2 compares a series of nested model specifications, shedding light on how out-of-sample performance evolves with model complexity. Specification A1 includes only a fixed intercept and is treated as a naive baseline.[23] The first real performance gain then comes in specification A4 where two-way (crossed) random intercepts are included. One-way random intercepts in the variety (A2) and region (A3) dimensions actually deteriorate out-of-sample performance relative to A1. This deterioration can be understood as a composition effect: When only one grouping factor is included, the model mistakes compositional differences (for example, in the distribution of grape varieties within and across regions) for genuine group effects. Including random effects in both the region and variety dimensions is crucial for disentangling these compositional differences.

[23]Specification A1 imposes that bud mortality is homogenous across cells.

Specifications A5-A7 then explore the incremental gains that can be achieved by supplementing specification A4 a variety of exposure- and acclimation-based covariates. Specification A5 highlights the importance of acclimation state proxies, with no discernible improvement in out-of-sample performance from including an exposure-based covariate on its own. Out-of-sample performance does improve, however, when a series of (state $\times$ exposure) interaction terms are included. Specification A6 focuses on a subset of acclimation state proxies that are likely to be available in most wine regions ($chill_r$ and $susceptibility_v$, which we refer to as group 1 state variables). This specification results in 0.7 and 0.9 percentage point reductions in the MAE of the primary and secondary bud mortality rate relative to specification A4. Additional performance gains are then achieved by specification A7 through the inclusion of higher-order interactions with acclimation state variables age_r and $disease_r$ (which we refer to as group 2 state variables). This final specification was used to produce the results in Sections 4.2 and 4.3.

4.4.2. *Alternative Temperature Thresholds.* Panel B of Figure 2 evaluates the sensitivity of our model's predictive performance to the selection of the fixed temperature threshold $\bar{T}$ used to compute our freeze severity index. These results reveal a modest but systematic reduction in out-of-sample predictive performance as this temperature threshold is increased. With $\bar{T} = -20°C$, our primary model specification (A7) achieves MAEs for the primary and secondary bud mortality rates of 4.9 and 8.4 percentage points, respectively. These figures increase by 0.4 percentage points (to 5.3 and 8.8 percentage points, respectively) when shifting to $\bar{T} = -17.5°C$ (B2) and by another 0.4 percentage points (to 5.7 and 9.2 percentage points, respectively) when shifting to $\bar{T} = -15°C$ (B1). Meanwhile, there is a modest (but diminishing) improvement in out-of-sample performance when shifting the threshold in the opposite direction. Under a threshold of $\bar{T} = -22.5°C$, the MAE of the primary and secondary bud mortality rates decreases to 4.6 and 7.8 percentage points, respectively. The MAE is unchanged (although there is a modest decrease in the RMSE of the secondary bud mortality rate of 0.1 percentage points) when decreasing the threshold by a further $2.5°C$ to $-25°C$. These modest differences across specifications are unsurprising given the cumulative nature of the freeze severity index.

4.4.3. *Alternative Covariates.* Panel C of Figure 2 assesses whether similar predictive performance can be achieved with alternative (but conceptually similar) covariates. Specification C1 replaces our cumulative measure of cold exposure with separate measures of the depth and duration of exposure, while specification C2 utilizes an alternative acclimation state covariate to proxy for chill accumulation. In both cases, there is only a modest deterioration in out-of-sample performance, with the MAE of the primary bud mortality rate increasing by only 0.6 and 0.3 percentage points for specifications C1 and C2, respectively.

4.4.4. *Random Slope Specifications.* Panel D explores whether random slopes could be incorporated into generalized linear mixed model specifications in lieu of acclimation state covariates. This is an important practical consideration since group 2 state covariates may be unavailable in some regions. The answer, however, is somewhat mixed. While random slopes do not improve out-of-sample performance in the complete absence of acclimation state variables (D1), they are able to deliver incremental gains when group 1 state variables are included in the model specification (D2). For instance, the MAE of the primary bud mortality rate decreases by 0.7 percentage points (to 5.7 percentage points) when shifting from specification A6 to specification D2, but falls short of the MAE of specification A7 (which achieves a MAE of 4.9 percentage points). However, when random intercepts are introduced on top of a more fulsome set of state covariates (as in specification D3), they are in fact counter-productive, resulting in a modest deterioration in out-of-sample performance relative to specification A7. Thus, while random slopes can deliver incremental gains when a comprehensive set of acclimation state variables are unavailable, it is not a silver bullet that can overcome a complete absence of acclimation state variables and they may in fact add noise when included on top of a more fulsome set of acclimation state variables.

Table 2. Out-of-sample performance of alternative first-stage model specifications.

	Primary		Secondary	
	MAE	RMSE	MAE	RMSE
Panel A: Nested Specifications				
(A1) Fixed Intercept	0.125	0.153	0.172	0.207
(A2) A1 with one-way random intercept (variety)	0.153	0.166	0.172	0.199
(A3) A1 with one-way random intercept (region)	0.135	0.164	0.174	0.206
(A4) A1 with two-way random intercept	0.071	0.086	0.118	0.129
(A5) A4 with $FSI_{r[i]}^{(\bar{T}=-20°C)}$	0.071	0.086	0.117	0.129
(A6) A5 with group 1 state interactions*	0.064	0.074	0.108	0.118
(A7) A6 with group 2 state interactions**	0.049	0.062	0.084	0.099
Panel B: Alternative Temperature Thresholds				
(B1) A7 but with $FSI_{r[i]}^{(\bar{T}=-15°C)}$ instead of $FSI_{r[i]}^{(\bar{T}=-20°C)}$	0.057	0.071	0.092	0.105
(B2) A7 but with $FSI_{r[i]}^{(\bar{T}=-17.5°C)}$ instead of $FSI_{r[i]}^{(\bar{T}=-20°C)}$	0.053	0.067	0.088	0.101
(B3) A7 but with $FSI_{r[i]}^{(\bar{T}=-22.5°C)}$ instead of $FSI_{r[i]}^{(\bar{T}=-20°C)}$	0.046	0.058	0.078	0.098
(B4) A7 but with $FSI_{r[i]}^{(\bar{T}=-25°C)}$ instead of $FSI_{r[i]}^{(\bar{T}=-20°C)}$	0.046	0.058	0.078	0.097
Panel C: Alternative Covariates				
(C1) A7 but with $depth_{r[i]}$ and $duration_{r[i]}$ instead of $FSI_{r[i]}^{(\bar{T}=-20°C)}$	0.055	0.068	0.100	0.117
(C2) A7 but with $utah_r$ instead of $chill_{r[i]}$	0.052	0.064	0.085	0.100
Panel D: Random Slope Specifications				
(D1) A5 with random slopes (region)	0.072	0.087	0.118	0.130
(D2) A6 with random slopes (region)	0.057	0.066	0.093	0.109
(D3) A7 with random slopes (region)	0.055	0.064	0.090	0.106

For more details on these model specifications, refer to Sections 4.1.5 and B.2.

* Group 1 state interactions include $susceptibility_{v[i]}$ and $chill_{r[i]}$.

** Group 2 state interactions include $age_{r[i]}$ and $disease_{r[i]}$.

5. Discussion

This paper proposes a fundamental shift to how grapevine bud mortality and production losses are computed after a cold event. Bud mortality surveys are routinely conducted after cold events in most developed wine regions and are used to compute direct estimates of bud mortality for each cell (recall: unique region-variety pair) via survey disaggregation. However, this methodology is unable to produce estimates for unsampled cells and will produce noisy estimates for sparsely sampled cells. These are major problems given the resource-intensive nature of collecting bud samples. In this paper, we show that multilevel regression and post-stratification (Gelman and Little (1997)) – a unit-level small area estimation technique that has been adopted across a wide range of domains (Molina (2024), Zhang et al. (2015), Lax and Phillips (2009)) – can be an effective tool for filling these informational gaps. By applying the methodology to a bud mortality survey conducted in British Columbia in 2023, we demonstrate that shifting to a model-based approach enables a dramatic improvement in modelling coverage relative to the status quo: reliable estimates are able to be produced for unsampled cells and estimates in sparsely sampled cells are subject to a smaller margin of error. The methodology also corrects for imbalances between the distribution of bud samples and production capacity across cells, allowing for more reliable estimates of production losses to be computed at the region, variety, and industry levels.

The estimates produced by our methodology are of practical use to a wide range of industry stakeholders. For wineries, cell-level estimates can be used to shed light on the anticipated impacts on their own operations and inform inventory management and pruning[24] decisions. This is particularly relevant for resource-constrained operations that are unable to conduct their own bud mortality surveys. These estimates can also help wineries situate themselves amongst their peers and identify if (and where) replacement grapes could be sourced from. For governments, our methodology's ability to produce reliable estimates of production losses at the industry level is critical for triggering government intervention well in advance of harvest. Once triggered, the more granular regional and varietal estimates are likely to be useful for designing these interventions and ensuring resources are allocated efficiently. These interventions may include emergency relief funding, tax exemptions, or temporary suspensions to regulatory restrictions on the importation of grapes from other regions.[25,26] For industry associations and retailers, early estimates of industry-wide production losses are critical for managing consumer expectations. And for insurance providers, these estimates

[24]Best practice guidelines suggest that pruning should be reduced in proportion to the primary bud mortality rate (Willwerth et al. (2014)).

[25]Product origin is closely controlled in most wine regions through appellation of origin programs and, in some regions, strictly prohibits the production of wine from imported grapes (Castriota (2020)).

[26]We note that all three of these interventions were implemented in British Columbia following a more severe cold event that wiped out nearly the entire the 2024 vintage.

may be useful for forecasting insurance payouts well in advance of when claims are filed, thus allowing them to manage their capital more efficiently in anticipation future payouts (Wang et al. (2021)).

Looking ahead, there are several opportunities for future research to advance this methodology. First, additional empirical applications are needed to further evaluate the methodology's performance. This could include applications in alternative geographic contexts to assess the extent to which the first-stage model specifications used in this paper generalize to other regions, as well as studies of cold events with more extreme probabilities of bud mortality (such as the cold event that plagued the 2024 vintage in British Columbia). There are also opportunities to extend this methodology across perennial crops more broadly. Second, there are opportunities to test alternative first-stage model specifications beyond those explored in this paper. For instance, recent work in the public opinion setting has evaluated the potential for alternative first-stage estimators – including stacked regression[27] (Ornstein (2020)) or Bayesian implementations that incorporate structured prior distributions on the random effects (Gao et al. (2021)) – to improve predictive performance. In the case of the latter, this could include specifying structured priors on the region and variety random effects that allow regions to partially pool toward those with similar levels of cold exposure and varieties to partially pool toward those with similar cold hardiness ratings.

[27]Ornstein (2020) proposes replacing the generalized linear mixed model in classical MRP with an ensemble model that consists of a generalized linear mixed model, random forest, gradient boosting, LASSO, and k nearest neighbours.

References

Anderson, K., Nelgen, S., and Pinilla, V. (2017). *Global wine markets, 1860 to 2016: a statistical compendium*. University of Adelaide Press. Accepted: 2018-01-11 23:55.

Ashenfelter, O. (2008). Predicting the Quality and Prices of Bordeaux Wine*. *The Economic Journal*, 118(529):F174–F184.

Ashenfelter, O., Ashmore, D., and Lalonde, R. (1995). Bordeaux Wine Vintage Quality and the Weather. *CHANCE*, 8(4):7–14.

Ashenfelter, O. and Storchmann, K. (2010a). Measuring the Economic Effect of Global Warming on Viticulture Using Auction, Retail, and Wholesale Prices. *Review of Industrial Organization*, 37(1):51–64.

Ashenfelter, O. and Storchmann, K. (2010b). Using hedonic models of solar radiation and weather to assess the economic effect of climate change: The case of Mosel Valley vineyards. *The Review of Economics and Statistics*, 92(2):333–349.

Ashenfelter, O. and Storchmann, K. (2016). Climate Change and Wine: A Review of the Economic Implications. *Journal of Wine Economics*, 11(1):105–138.

Barriguinha, A., de Castro Neto, M., and Gil, A. (2021). Vineyard Yield Estimation, Prediction, and Forecasting: A Systematic Literature Review. *Agronomy*, 11(9):1789.

Bates, D., Maechler, M., Bolker, B., and Walker, S. (2003). lme4: Linear Mixed-Effects Models using 'Eigen' and S4. Institution: Comprehensive R Archive Network Pages: 1.1-37.

Battese, G. E., Harter, R. M., and Fuller, W. A. (1988). An Error-Components Model for Prediction of County Crop Areas Using Survey and Satellite Data. *Journal of the American Statistical Association*, 83(401):28–36.

Beckert, J., Rössel, J., and Schenk, P. (2017). Wine as a Cultural Product: Symbolic Capital and Price Formation in the Wine Field. *Sociological Perspectives*, 60(1):206–222.

Berelowitz, L. (2023). British Columbia's wine industry facing major climate-change challenges. *Decanter*. Section: Wine News.

Breslow, N. E. and Clayton, D. G. (1993). Approximate Inference in Generalized Linear Mixed Models. *Journal of the American Statistical Association*, 88(421):9–25.

British Columbia Wine Grape Council (2025). Annual Crop Assessment.

Bucheli, J., Conrad, N., Wimmer, S., Dalhaus, T., and Finger, R. (2023). Weather insurance in European crop and horticulture production. *Climate Risk Management*, 41:100525.

Buttice, M. K. and Highton, B. (2013). How Does Multilevel Regression and Poststratification Perform with Conventional National Surveys? *Political Analysis*, 21(4):449–467.

Byron, R. P. and Ashenfelter, O. (1995). Predicting the Quality of an Unborn Grange*. *Economic Record*, 71(1):40–53.

Castriota, S. (2020). *Wine Economics*. MIT Press, Cambridge, MA, USA.

Chang, B.-M., Estergaard, B., and Marsh, S. (2024). Warmer but Longer Cold Air Exposure Can Hurt. In *2024 American Society for Enology and Viticulture National Conference*, Oregon, USA. American Society for Enology and Viticulture.

Clingeleffer, P., Martin, S., Dunn, G., and Krstic, M. (2001). Crop development, crop estimation and crop control to secure quality and production of major wine grape varieties: a national approach. Technical report, Grape and Wine Research & Development Corporation, Adelaide, Australia.

Corral, P., Cojocaru, A., Segovia, S., and Molina, I. (2022). *Guidelines to Small Area Estimation for Poverty Mapping*. World Bank, Washington, DC.

Corsi, A. and Ashenfelter, O. (2019). Predicting Italian Wine Quality from Weather Data and Expert Ratings. *Journal of Wine Economics*, 14(3):234–251.

Cunha, M., Abreu, I., Pinto, P., and Castro, R. d. (2003). Airborne Pollen Samples for Early-Season Estimates of Wine Production in a Mediterranean Climate Area of Northern Portugal. *American Journal of Enology and Viticulture*, 54(3):189–194.

Cunha, M., Marçal, A. R. S., and Silva, L. (2010). Very early prediction of wine yield based on satellite data from vegetation. *International Journal of Remote Sensing*, 31(12):3125–3142.

Cunha, M., Ribeiro, H., and Abreu, I. (2016). Pollen-based predictive modelling of wine production: application to an arid region. *European Journal of Agronomy*, 73:42–54.

Dami, I. E., Ennahli, S., and Zhang, Y. (2012). Assessment of Winter Injury in Grape Cultivars and Pruning Strategies Following a Freezing Stress Event. *American Journal of Enology and Viticulture*, 63(1):106–111.

Dobrei, A., Dobrei, l., Posta, G., Danci, M., Nistor, E., Camen, D., Mălăescu, M., and Sala, F. (2016). Research Concerning the Correlation between Crop Load, Leaf Area and Grape Yield in Few Grapevine Varieties. *Agriculture and Agricultural Science Procedia*, 10:222–232.

Erciulescu, A. L., Cruze, N. B., and Nandram, B. (2019). Model-Based County Level Crop Estimates Incorporating Auxiliary Sources of Information. *Journal of the Royal Statistical Society Series A: Statistics in Society*, 182(1):283–303.

Esau, D., Rowan, A., Barnhardt, G., and King, R. (2024). Grape Gap Analysis. Technical report, British Columbia Ministry of Agriculture and Food.

Falcó, J. M., Marco-Lajara, B., Sánchez-García, E., and Jr, A. G. (2023). The Economic, Social, and Environmental Value of the Spanish Wine Industry. In *Handbook of Research on Sustainability Challenges in the Wine Industry*, pages 169–193. IGI Global Scientific Publishing.

Faust, E. and Herbold, J. (2018). Spring frost losses and climate change – Not a contradiction in terms.

Fennell, A. (2004). Freezing Tolerance and Injury in Grapevines. *Journal of Crop Improvement*, 10(1-2):201–235. _eprint: https://doi.org/10.1300/J411v10n01_09.

Ferguson, J. C., Moyer, M. M., Mills, L. J., Hoogenboom, G., and Keller, M. (2014). Modeling Dormant Bud Cold Hardiness and Budbreak in Twenty-Three Vitis Genotypes Reveals Variation by Region of Origin. *American Journal of Enology and Viticulture*, 65(1):59–71.

Ferguson, J. C., Tarara, J. M., Mills, L. J., Grove, G. G., and Keller, M. (2011). Dynamic thermal time model of cold hardiness for dormant grapevine buds. *Annals of Botany*, 107(3):389–396.

Fish, T. and Romano, A. (2022). Late-Spring Frost Imperils Oregon and California Vineyards. *Wine Spectator*.

Gao, Y., Kennedy, L., Simpson, D., and Gelman, A. (2021). Improving Multilevel Regression and Poststratification with Structured Priors. *Bayesian Analysis*, 16(3):719–744.

Gelman, A. and Hill, J. (2007). *Data Analysis Using Regression and Multilevel/Hierarchical Models*. Cambridge University Press. Google-Books-ID: lV3DIdV0F9AC.

Gelman, A. and Little, T. C. (1997). Poststratification into Many Categories Using Hierarchical Logistic Regression. *Survey Methodology*, 23(2):127–135. Pages: 127 Publication Title: Survey Methodology Volume: 23.

Haddad, E., Aroca, P., Jano, P., Rocha, A., and Pimenta, B. (2020). A Bad Year? Climate Variability and the Wine Industry in Chile. *Wine Economics and Policy*, 9(2):23–35.

Haeger, J. W. and Storchmann, K. (2006). Prices of American Pinot Noir wines: climate, craftsmanship, critics. *Agricultural Economics*, 35(1):67–78.

Harding, J. and Robinson, J. (2015). *The Oxford Companion to Wine*. Oxford University Press.

Howe, P. D., Mildenberger, M., Marlon, J. R., and Leiserowitz, A. (2015). Geographic variation in opinions on climate change at state and local scales in the USA. *Nature Climate Change*, 5(6):596–603.

Howell, G. S. (2001). Sustainable Grape Productivity and the Growth-Yield Relationship: A Review. *American Journal of Enology and Viticulture*, 52(3):165–174.

Howell, S. (1988). Cultural manipulation of vine cold hardiness. In *In Proceedings of the Second International Cool Climate Symposium for Viticulture and Oenology*, pages 98–102, Auckland. New Zealand Society for Viticulture and Oenology.

Intergovernmental Panel On Climate Change (IPCC) (2023). *Climate Change 2021 – The Physical Science Basis: Working Group I Contribution to the Sixth Assessment Report of the Intergovernmental Panel on Climate Change*. Cambridge University Press, 1 edition.

Jaramillo, J., Vanden Heuvel, J., and Petersen, K. H. (2021). Low-Cost, Computer Vision-Based, Prebloom Cluster Count Prediction in Vineyards. *Frontiers in Agronomy*, 3.

Jones, G. V., White, M. A., Cooper, O. R., and Storchmann, K. (2005). Climate Change and Global Wine Quality. *Climatic Change*, 73(3):319–343.

Kaya, O., Delavar, H., Shikanai, A., Auwarter, C., and Hatterman-Valenti, H. (2024). Assessing the influence of autumnal temperature fluctuations on cold hardiness in different grapevine cultivars: variations across vine age and bud positions. *Frontiers in Plant Science*, 15.

Keller, M. (2020). *The Science of Grapevines*. Academic Press. Google-Books-ID: g_zLDwAAQBAJ.

Kong, A. Y. and Zhang, X. (2020). The Use of Small Area Estimates in Place-Based Health Research. *American Journal of Public Health*, 110(6):829–832.

Kovaleski, A. P., North, M. G., Martinson, T. E., and Londo, J. P. (2023). Development of a new cold hardiness prediction model for grapevine using phased integration of acclimation and deacclimation responses. *Agricultural and Forest Meteorology*, 331:109324.

Lange, S., Pape, U. J., and Pütz, P. (2022). Small Area Estimation of Poverty Under Structural Change. *Review of Income and Wealth*, 68(S2):S264–S281. _eprint: https://onlinelibrary.wiley.com/doi/pdf/10.1111/roiw.12558.

Laurent, C., Oger, B., Taylor, J. A., Scholasch, T., Metay, A., and Tisseyre, B. (2021). A review of the issues, methods and perspectives for yield estimation, prediction and forecasting in viticulture. *European Journal of Agronomy*, 130:126339.

Lax, J. R. and Phillips, J. H. (2009). How Should We Estimate Public Opinion in The States? *American Journal of Political Science*, 53(1):107–121.

Londo, J. and Kovaleski, A. (2019). Deconstructing cold hardiness: variation in supercooling ability and chilling requirements in the wild grapevine Vitis riparia. *Australian Journal of Grape and Wine Research*, 25(3):276–285. _eprint: https://onlinelibrary.wiley.com/doi/pdf/10.1111/ajgw.12389.

Londo, J. P. and Kovaleski, A. P. (2025). Integrating cold hardiness and deacclimation resistance demonstrates a conserved response to chilling accumulation in grapevines. *Journal of Experimental Botany*, 76(11):3158–3171.

Martinson, T., Walet-Peterson, H., Haggerty, L., O'Connell, J., and Colizzi, M. (2014). Finger Lakes Vineyard Update: Winter Injury 2014 Wrap Up. Technical report, Cornell University Cooperative Extension, Finger Lakes Grape Program.

McMaster, G. S. and Wilhelm, W. W. (1997). Growing degree-days: one equation, two interpretations. *Agricultural and Forest Meteorology*, 87(4):291–300.

Meier, M., Fuhrer, J., and Holzkämper, A. (2018). Changing risk of spring frost damage in grapevines due to climate change? A case study in the Swiss Rhone Valley. *International Journal of Biometeorology*, 62(6):991–1002.

Menne, M. J., Noone, S., Casey, N. W., Dunn, R. H., McNeill, S., Kantor, D., Thorne, P. W., Orcutt, K., Cunningham, S., and Risavi, N. (2023). Global Historical Climatology Network-Hourly (GHCNh). NOAA National Centers for Environmental Information.

Mercer, C. (2021). Update: €1bn aid for frost-hit French vineyards and farmers. *Decanter*. Section: Wine News.

Mercer, C. (2024). Frost damage in German vineyards to cost millions. *Decanter*. Section: Wine News.

Merot, A., Metay, A., Smits, N., and Thiollet-Scholtus, M. (2022). Adaptation of the regional agronomic diagnosis for grapevine yield analysis. *OENO One*, 56(1):87–99.

Mills, L. J., Ferguson, J. C., and Keller, M. (2006). Cold-Hardiness Evaluation of Grapevine Buds and Cane Tissues. *American Journal of Enology and Viticulture*, 57(2):194–200.

Molina, I. (2024). *Frontiers in Small Area Estimation Research: Application to Welfare Indicators*. World Bank, Washington, DC.

Molina, I. and Rao, J. N. K. (2010). Small area estimation of poverty indicators. *Canadian Journal of Statistics*, 38(3):369–385. _eprint: https://onlinelibrary.wiley.com/doi/pdf/10.1002/cjs.10051.

Molitor, D., Caffarra, A., Sinigoj, P., Pertot, I., Hoffmann, L., and Junk, J. (2014). Late frost damage risk for viticulture under future climate conditions: a case study for the Luxembourgish winegrowing region. *Australian Journal of Grape and Wine Research*, 20(1):160–168. _eprint: https://onlinelibrary.wiley.com/doi/pdf/10.1111/ajgw.12059.

Mosedale, J. R., Wilson, R. J., and Maclean, I. M. D. (2015). Climate Change and Crop Exposure to Adverse Weather: Changes to Frost Risk and Grapevine Flowering Conditions. *PLOS ONE*, 10(10):e0141218.

Niklas, B. (2017). Impact of Annual Weather Fluctuations on Wine Production in Germany. *Journal of Wine Economics*, 12(4):436–445.

Nuske, S., Wilshusen, K., Achar, S., Yoder, L., Narasimhan, S., and Singh, S. (2014). Automated Visual Yield Estimation in Vineyards. *Journal of Field Robotics*, 31(5):837–860.

Oczkowski, E. (2016). The Effect of Weather on Wine Quality and Prices: An Australian Spatial Analysis. *Journal of Wine Economics*, 11(1):48–65.

Ornstein, J. T. (2020). Stacked Regression and Poststratification. *Political Analysis*, 28(2):293–301.

Pacheco, J. (2011). Using National Surveys to Measure Dynamic U.S. State Public Opinion: A Guideline for Scholars and an Application. *State Politics & Policy Quarterly*, 11(4):415–439.

Pierquet, P. and Stushnoff, C. (1980). Relationship of Low Temperature Exotherms to Cold Injury in Vitis Riparia Michx. *American Journal of Enology and Viticulture*, 31(1):1–6.

Pratt, C. (1974). Vegetative Anatomy of Cultivated Grapes–A Review. *American Journal of Enology and Viticulture*, 25(3):131–150.

Puga, G. and Anderson, K. (2024). Winegrape Yield and Revenue Variability in Australia. *Australian Journal of Grape and Wine Research*, 2024(1):9992528. _eprint: https://onlinelibrary.wiley.com/doi/pdf/10.1155/2024/9992528.

Puga, G. and Anderson, K. (2025a). How Can We Use Econometrics to Assess Climate Impacts on the Wine Industry? *Harvard Data Science Review*, 7(2).

Puga, G. and Anderson, K. (2025b). Statistical methods in grape and wine research for quantifying the impact of climate change. *OENO One*, 59(1).

Puga, G., Anderson, K., and Tchatoka, F. D. (2023). The impact of climate change on grape yields: Evidence from Australia. *OENO One*, 57(2).

Quamme, H. (1986). Use of thermal analysis to measure freezing resistance of grape buds. *Canadian Journal of Plant Science*, 66(4):947–952.

Quamme, H. A. (1974). An Exothermic Process Involved in the Freezing Injury to Flower Buds of Several Prunus Species. *Journal of the American Society for Horticultural Science*, 99(4):315–318.

Rahman, A. (2017). Estimating small area health-related characteristics of populations: a methodological review. *Geospatial Health*, 12(1).

Richardson, A. E., Seeley, S., and Walker, D. (1974). A Model for Estimating the Completion of Rest for 'Redhaven' and 'Elberta' Peach Trees. *HortScience*, 9(4):331–332.

Santos, J. A., Ceglar, A., Toreti, A., and Prodhomme, C. (2020). Performance of seasonal forecasts of Douro and Port wine production. *Agricultural and Forest Meteorology*, 291:108095.

Santos, J. A., Grätsch, S. D., Karremann, M. K., Jones, G. V., and Pinto, J. G. (2013). Ensemble projections for wine production in the Douro Valley of Portugal. *Climatic Change*, 117(1):211–225.

Santos, J. A., Malheiro, A. C., Karremann, M. K., and Joaquim G. Pinto (2011). Statistical modelling of grapevine yield in the Port Wine region under present and future climate conditions. *International Journal of Biometeorology*, 55(2):119–131.

Saxena, A., Paola Pesantez-Cabrera, Ballapragada, R., Lam, K.-H., Keller, M., and Fern, A. (2023). Grape Cold Hardiness Prediction via Multi-Task Learning. *Proceedings of the AAAI Conference on Artificial Intelligence*, 37(13):15717–15723.

Schultz, H. R. (2016). Global Climate Change, Sustainability, and Some Challenges for Grape and Wine Production. *Journal of Wine Economics*, 11(1):181–200.

Sgubin, G., Swingedouw, D., Dayon, G., García de Cortázar-Atauri, I., Ollat, N., Pagé, C., and van Leeuwen, C. (2018). The risk of tardive frost damage in French vineyards in a changing climate. *Agricultural and Forest Meteorology*, 250-251:226–242.

Smith, S. C. and Alston, J. M. (2024). CLIMATE, WEATHER, AND COLLECTIVE REPUTATION: IMPLICATIONS FOR CALIFORNIA'S WINE PRICES AND QUALITY. *American Association of Wine Economists (AAWE) Working Paper Series*.

Storchmann, K. (2012). Wine Economics. *Journal of Wine Economics*, 7(1):1–33.

Storchmann, K. and Cao, J. (2025). Wine Economics: Emergence, Topics, and Outlook. *Harvard Data Science Review*, 7(1).

Urbez-Torres, J. R. (2016). Demystifying the status of grapevine viruses in British Columbia.

VineTech Canada (2025). Frost Ratings.

Wample, R. and Wolf, T. (1997). Practical considerations that impact vine cold hardiness. In *Proceedings of the fourth international symposium on cool climate viticulture & enology*, Rochester, NY.

Wang, H. and Londo, J. P. (2025). VineColD: an integrative database for global historical tracing and real-time monitoring of grapevine cold hardiness. *Database: The Journal of Biological Databases and Curation*, 2025:baaf055.

Wang, H., Moghe, G. D., Kovaleski, A. P., Keller, M., Martinson, T. E., Wright, A. H., Franklin, J. L., Hébert-Haché, A., Provost, C., Reinke, M., Atucha, A., North, M. G., Russo, J. P., Helwi, P., Centinari, M., and Londo, J. P. (2024). NYUS.2: an automated machine learning prediction model for the large-scale real-time simulation of grapevine freezing tolerance in North America. *Horticulture Research*, 11(2):uhad286.

Wang, Z., Wu, X., and Qiu, C. (2021). THE IMPACTS OF INDIVIDUAL INFORMATION ON LOSS RESERVING. *ASTIN Bulletin: The Journal of the IAA*, 51(1):303–347.

Weinberger, J. (1950). Chilling requirements of peach varieties. *Proceedings of the American Society for Horticultural Science*, 56.

Willwerth, J., Ker, K., and Inglis, D. (2014). Best Management Practices for Reducing Winter Injury in Grapevines. Technical report, Cool Climate Oenology & Viticulture Institute, Brock University, St. Catherines, Ontario.

Wolfe, W. (2001). Vine and vineyard management following low temperature injury. In *Proceedings of the ASEV 50th Anniversary Annual Meeting*, pages 101–110. American Society for Enology and Viticulture, Davis.

Zabadal, T. J., Dami, I. E., Goffinet, M. C., Martinson, T. E., and Mark L. Chien (2007). Winter Injury to Grapevines and Methods of Protection. Technical Report E2930, Michigan State University.

Zhang, X., Holt, J. B., Yun, S., Lu, H., Greenlund, K. J., and Croft, J. B. (2015). Validation of Multilevel Regression and Poststratification Methodology for Small Area Estimation of Health Indicators From the Behavioral Risk Factor Surveillance System. *American Journal of Epidemiology*, 182(2):127–137.

Appendix A. Supplementary Tables & Figures

Table A.1. Summary Statistics

Statistic	n	Min	Mean	Median	Max	St. Dev.
$FSI_{(\bar{T}=-25°C)}$	401	0	20.7	0	68.8	24.8
$FSI_{(\bar{T}=-22.5°C)}$	401	0	49.9	13.8	147.3	56.3
$FSI_{(\bar{T}=-20°C)}$	401	4.1	108.9	50.2	372.4	112.3
$FSI_{(\bar{T}=-17.5°C)}$	401	34.2	225.6	136.2	646.7	189.4
$FSI_{(\bar{T}=-15°C)}$	401	124.5	425.7	337.0	959.1	265.7
depth	401	-30.8	-25.5	-24.2	-21.3	3.7
duration	401	6	33	19	102	27.0
chill	401	212	565	640	723	157.4
susceptibility	401	1.00	5.89	6.00	10.00	2.19
age	401	0.000	0.095	0.073	0.224	0.067
disease	401	0.120	0.467	0.620	0.670	0.228
Counterfactual production capacity (tons)	401	1.0	114.0	16.0	4,755.0	360.6

Note: Summary statistics are computed across cells.

Table A.2. Cold Hardiness by Variety

Cold Hardiness Scale	Variety(s)
1	Concord, Elvira, Fredonia, Frontenac, Frontenac Gris, Leon Millot, Marquette, Marechal Foch
2	De Chaunac, Sovereign Opal, Traminette
3	Baco Noir, Seyval Blanc, Aurore, Cayuga White, Geisenheim 318, Niagara, Vidal, Regent
4	Chambourcin, Kerner, Dornfelder, Zweigeltrebe
5	Cabernet Franc, Gamay Noir, Riesling, Aligote, Petit Verdot
6	Chardonnay, Pinot Noir, Muscat, Auxerrois, Cabernet Sauvignon, Pinot Blanc, Pinot Gris
7	Malbec, Viognier
8	Syrah, Semillon, Chenin Blanc, Limberger, Gewurz-traminer
9	Merlot
10	Zinfandel, Petit Sirah, Nebbiolo, Sauvignon Blanc

Source: Product characteristics, VineTech Canada (2025)

Appendix B. Supplementary Technical Information

B.1. **Assignment of Hourly Temperature Data from Weather Stations to Wine-Producing Regions.** As noted in Section 4.1.2, hourly temperature data was obtained for 78 weather stations in Southern British Columbia, with 54 stations retained after applying a minimum completeness criterion. Temperature observations were then mapped to British Columbia's wine-producing regions in R by the following point-to-polygon spatial transformation. First, we construct Thiessen (or Voronoi) polygons using the point coordinates of weather stations as an input. These polygons identify the area surrounding each weather station that contains all coordinates closer to that weather station than any other weather station in the dataset. Second, we perform a spatial join between the Thiessen polygons and the boundaries of the wine-producing regions. This forms a larger set of smaller polygons – which we will call 'joined polygons' – that map to exactly 1 weather station and 1 region. Finally, the hourly temperature within region r at time t (denoted by $T_{r,t}$) is computed by taking the area-based weighted average of the hourly temperatures of joined polygons i within region r at time t (denoted by $T_{i,t}$):

$$T_{r,t} = \frac{\sum_{i \in I_r} Area_i \times T_{i,t}}{Area_r} \tag{17}$$

where $Area_i$ is the area of joined polygon i, $Area_r$ is the area of region r, and I_r is the set of joined polygons i in region r.

B.2. **List of Alternative First-Stage Model Specifications.** This section provides a complete breakdown of the alternative model specifications introduced in Section 4.1.5 and reported in Section 4.4. In each of the specifications listed below, α_r and α_v are modelled as being drawn from a normal distribution with mean zero and variances σ_r^2 and σ_v^2, respectively.

$$Pr(m_{i,r[i],v[i]}) = logit^{-1}(\alpha) \quad \text{for} \quad i = 1, ..., N \tag{A1}$$

$$Pr(m_{i,r[i],v[i]}) = logit^{-1}(\alpha + \alpha_{v[i]}) \quad \text{for} \quad i = 1, ..., N \tag{A2}$$

$$Pr(m_{i,r[i],v[i]}) = logit^{-1}(\alpha + \alpha_{r[i]}) \quad \text{for} \quad i = 1, ..., N \tag{A3}$$

$$Pr(m_{i,r[i],v[i]}) = logit^{-1}(\alpha + \alpha_{v[i]} + \alpha_{r[i]}) \quad \text{for} \quad i = 1, ..., N \tag{A4}$$

$$Pr(m_{i,r[i],v[i]}) = logit^{-1}(\alpha + \alpha_{v[i]} + \alpha_{r[i]} + \beta_1 FSI_{r[i]}) \quad \text{for} \quad i = 1, ..., N \tag{A5}$$

$$\begin{aligned} Pr(m_{i,r[i],v[i]}) = logit^{-1}(&\alpha + \alpha_{v[i]} + \alpha_{r[i]} + \beta_1 FSI_{r[i]} + \\ &\beta_2(FSI_{r[i]} \times susceptibility_{v[i]} \times chill_{r[i]})) \\ &\text{for} \quad i = 1, ..., N \end{aligned} \tag{A6}$$

$$\begin{aligned} Pr(m_{i,r[i],v[i]}) = logit^{-1}(&\alpha + \alpha_{r[i]} + \alpha_{v[i]} + \beta_1 FSI_{r[i]} + \\ &\beta_2(FSI_{r[i]} \times chill_{r[i]} \times susceptibility_{v[i]}) + \\ &\beta_3(FSI_{r[i]} \times chill_{r[i]} \times susceptibility_{v[i]} \times age_{r[i]}) + \\ &\beta_4(FSI_{r[i]} \times chill_{r[i]} \times susceptibility_{v[i]} \times disease_{r[i]}) + \\ &\beta_5(FSI_{r[i]} \times chill_{r[i]} \times susceptibility_{v[i]} \times age_{r[i]} \times disease_{r[i]})) \\ &\text{for} \quad i = 1, ..., N \end{aligned} \tag{A7}$$

$$\begin{aligned} Pr(m_{i,r[i],v[i]}) = logit^{-1}(&\alpha + \alpha_{r[i]} + \alpha_{v[i]} + \beta_1 FSI_{r[i]}^{(\bar{T}=-15°C)} + \\ &\beta_2(FSI_{r[i]}^{(\bar{T}=-15°C)} \times chill_{r[i]} \times susceptibility_{v[i]}) + \\ &\beta_3(FSI_{r[i]}^{(\bar{T}=-15°C)} \times chill_{r[i]} \times susceptibility_{v[i]} \times age_{r[i]}) + \\ &\beta_4(FSI_{r[i]}^{(\bar{T}=-15°C)} \times chill_{r[i]} \times susceptibility_{v[i]} \times disease_{r[i]}) + \\ &\beta_5(FSI_{r[i]}^{(\bar{T}=-15°C)} \times chill_{r[i]} \times susceptibility_{v[i]} \times age_{r[i]} \times disease_{r[i]})) \\ &\text{for} \quad i = 1, ..., N \end{aligned} \tag{B1}$$

$$\begin{aligned} Pr(m_{i,r[i],v[i]}) = logit^{-1}(&\alpha + \alpha_{r[i]} + \alpha_{v[i]} + \beta_1 FSI_{r[i]}^{(\bar{T}=-17.5°C)} + \\ &\beta_2(FSI_{r[i]}^{(\bar{T}=-17.5°C)} \times chill_{r[i]} \times susceptibility_{v[i]}) + \\ &\beta_3(FSI_{r[i]}^{(\bar{T}=-17.5°C)} \times chill_{r[i]} \times susceptibility_{v[i]} \times age_{r[i]}) + \\ &\beta_4(FSI_{r[i]}^{(\bar{T}=-17.5°C)} \times chill_{r[i]} \times susceptibility_{v[i]} \times disease_{r[i]}) + \\ &\beta_5(FSI_{r[i]}^{(\bar{T}=-17.5°C)} \times chill_{r[i]} \times susceptibility_{v[i]} \times age_{r[i]} \times disease_{r[i]})) \\ &\text{for} \quad i = 1, ..., N \end{aligned} \tag{B2}$$

$$
\begin{aligned}
Pr(m_{i,r[i],v[i]}) = \; & logit^{-1}(\alpha + \alpha_{r[i]} + \alpha_{v[i]} + \beta_1 FSI_{r[i]}^{(\bar{T}=-22.5^\circ C)} + \\
& \beta_2(FSI_{r[i]}^{(\bar{T}=-22.5^\circ C)} \times chill_{r[i]} \times susceptibility_{v[i]}) + \\
& \beta_3(FSI_{r[i]}^{(\bar{T}=-22.5^\circ C)} \times chill_{r[i]} \times susceptibility_{v[i]} \times age_{r[i]}) + \\
& \beta_4(FSI_{r[i]}^{(\bar{T}=-22.5^\circ C)} \times chill_{r[i]} \times susceptibility_{v[i]} \times disease_{r[i]}) + \\
& \beta_5(FSI_{r[i]}^{(\bar{T}=-22.5^\circ C)} \times chill_{r[i]} \times susceptibility_{v[i]} \times age_{r[i]} \times disease_{r[i]})) \\
& \text{for} \quad i = 1, ..., N
\end{aligned}
\tag{B3}
$$

$$
\begin{aligned}
Pr(m_{i,r[i],v[i]}) = \; & logit^{-1}(\alpha + \alpha_{r[i]} + \alpha_{v[i]} + \beta_1 FSI_{r[i]}^{(\bar{T}=-25^\circ C)} + \\
& \beta_2(FSI_{r[i]}^{(\bar{T}=-25^\circ C)} \times chill_{r[i]} \times susceptibility_{v[i]}) + \\
& \beta_3(FSI_{r[i]}^{(\bar{T}=-25^\circ C)} \times chill_{r[i]} \times susceptibility_{v[i]} \times age_{r[i]}) + \\
& \beta_4(FSI_{r[i]}^{(\bar{T}=-25^\circ C)} \times chill_{r[i]} \times susceptibility_{v[i]} \times disease_{r[i]}) + \\
& \beta_5(FSI_{r[i]}^{(\bar{T}=-25^\circ C)} \times chill_{r[i]} \times susceptibility_{v[i]} \times age_{r[i]} \times disease_{r[i]})) \\
& \text{for} \quad i = 1, ..., N
\end{aligned}
\tag{B4}
$$

$$
\begin{aligned}
Pr(m_{i,r[i],v[i]}) = \; & logit^{-1}(\alpha + \alpha_{r[i]} + \alpha_{v[i]} + \beta_1 depth_{r[i]} + \beta_2 duration_{r[i]} + \\
& \beta_3(depth_{r[i]} \times chill_{r[i]} \times susceptibility_{v[i]}) + \\
& \beta_4(depth_{r[i]} \times chill_{r[i]} \times susceptibility_{v[i]} \times age_{r[i]}) + \\
& \beta_5(depth_{r[i]} \times chill_{r[i]} \times susceptibility_{v[i]} \times disease_{r[i]}) + \\
& \beta_6(depth_{r[i]} \times chill_{r[i]} \times susceptibility_{v[i]} \times age_{r[i]} \times disease_{r[i]})) \\
& \beta_7(duration_{r[i]} \times chill_{r[i]} \times susceptibility_{v[i]}) + \\
& \beta_8(duration_{r[i]} \times chill_{r[i]} \times susceptibility_{v[i]} \times age_{r[i]}) + \\
& \beta_9(duration_{r[i]} \times chill_{r[i]} \times susceptibility_{v[i]} \times disease_{r[i]}) + \\
& \beta_{10}(duration_{r[i]} \times chill_{r[i]} \times susceptibility_{v[i]} \times age_{r[i]} \times disease_{r[i]})) \\
& \text{for} \quad i = 1, ..., N
\end{aligned}
\tag{C1}
$$

$$\begin{aligned} Pr(m_{i,r[i],v[i]}) = \; & logit^{-1}(\alpha + \alpha_{r[i]} + \alpha_{v[i]} + \beta_1 FSI_{r[i]} + \\ & \beta_2(FSI_{r[i]} \times utah_{r[i]} \times susceptibility_{v[i]}) + \\ & \beta_3(FSI_{r[i]} \times utah_{r[i]} \times susceptibility_{v[i]} \times age_{r[i]}) + \\ & \beta_4(FSI_{r[i]} \times utah_{r[i]} \times susceptibility_{v[i]} \times disease_{r[i]}) + \\ & \beta_5(FSI_{r[i]} \times utah_{r[i]} \times susceptibility_{v[i]} \times age_{r[i]} \times disease_{r[i]})) \\ & \text{for} \quad i = 1, ..., N \end{aligned} \tag{C2}$$

$$\begin{aligned} Pr(m_{i,r[i],v[i]} = 1) = \; & logit^{-1}(\alpha + \alpha_{r[i]} + \alpha_{v[i]} + \beta_1 FSI_{r[i]} + \beta_{1,r[i]} FSI_{r[i]}) \\ & \text{for} \quad i = 1, ..., N \end{aligned} \tag{D1}$$

$$\begin{aligned} Pr(m_{i,r[i],v[i]} = 1) = \; & logit^{-1}(\alpha + \alpha_{r[i]} + \alpha_{v[i]} + \\ & \beta_1 FSI_{r[i]} + \\ & \beta_{1,r[i]} FSI_{r[i]} \\ & \beta_2(FSI_{r[i]} \times chill_{r[i]} \times susceptibility_{v[i]}) \\ & \beta_{2,r[i]}(FSI_{r[i]} \times chill_{r[i]} \times susceptibility_{v[i]})) \\ & \text{for} \quad i = 1, ..., N \end{aligned} \tag{D2}$$

$$\begin{aligned} Pr(m_{i,r[i],v[i]}) = \; & logit^{-1}(\alpha + \alpha_{r[i]} + \alpha_{v[i]} + \\ & \beta_1 FSI_{r[i]} + \\ & \beta_{1,r[i]} FSI_{r[i]} + \\ & \beta_2(FSI_{r[i]} \times chill_{r[i]} \times susceptibility_{v[i]}) + \\ & \beta_{2,r[i]}(FSI_{r[i]} \times chill_{r[i]} \times susceptibility_{v[i]})) \\ & \beta_3(FSI_{r[i]} \times chill_{r[i]} \times susceptibility_{v[i]} \times age_{r[i]}) + \\ & \beta_{3,r[i]}(FSI_{r[i]} \times chill_{r[i]} \times susceptibility_{v[i]} \times age_{r[i]}) + \\ & \beta_4(FSI_{r[i]} \times chill_{r[i]} \times susceptibility_{v[i]} \times disease_{r[i]}) + \\ & \beta_{4,r[i]}(FSI_{r[i]} \times chill_{r[i]} \times susceptibility_{v[i]} \times disease_{r[i]}) + \\ & \beta_5(FSI_{r[i]} \times chill_{r[i]} \times susceptibility_{v[i]} \times age_{r[i]} \times disease_{r[i]})) \\ & \beta_{5,r[i]}(FSI_{r[i]} \times chill_{r[i]} \times susceptibility_{v[i]} \times age_{r[i]} \times disease_{r[i]})) \\ & \text{for} \quad i = 1, ..., N \end{aligned} \tag{D3}$$

B.3. **List of Cells Used for Model Validation.** Model validation is based on a subset of cells for which direct estimates of bud mortality could be produced via survey disaggregation that are subject to a relatively small degree of sampling error. We set this threshold at 500 samples, resulting in a validation set of 13 cells spanning 3 regions and 9 varieties. These cells are listed in Table A.3.

Table A.3. List of Cells Used for Model Validation ($n \geq 500$)

Region	Variety	Secondary Bud Samples	Primary Bud Samples
Oliver	Merlot	3,328	3,328
Oliver	Pinot Noir	1,983	1,982
Oliver	Pinot Gris	1,853	1,853
Oliver	Chardonnay	1,758	1,758
Oliver	Cabernet Franc	1,363	1,363
Oliver	Syrah	1,054	1,054
Oliver	Cabernet Sauvignon	896	896
Osoyoos	Merlot	776	776
Oliver	Sauvignon Blanc	744	743
Osoyoos	Cabernet Franc	600	600
Kelowna	Pinot Gris	565	565
Kelowna	Pinot Noir	550	550
Oliver	Gewurztraminer	542	542